Design and Simulation of Magnetic Thrust and Radial Bearing System

Dissertation for the degree of

Master by Research

Kingston University

2016

Presented by

Arpi Shah

Acknowledgements

This thesis is the result of the work I carried out at the Kingston University's Roehampton vale campus. I would like to express my heartfelt gratitude to those who made this work possible

The first person I would like to thank is my main supervisor Prof Mehmet Necip Sahinkaya, for giving me the opportunity to work on this project, for being a constant inspiration throughout my research project, and for what I learned from him about providing highest quality of work. I am greatly profited from his enthusiastic and critical observation on research. I feel very fortunate and honoured to have had the opportunity to learn and work with him.

I cannot be thankful enough to Dr Mohamad Askari of whom I had excellent guidance and advice during experimental work. His time, constructive criticism and encouragement have likewise resulted in the present dissertation, I truly thank for his invaluable comments, suggestions and discussions during the whole work with this thesis.

I would like to express gratefulness to Science, Engineering, and computer research team for organising valuable training session for research student and for finical support.

I would like to thank all employees, working in university lab for their help for the realization of the test rig.

Last but not least, a special thanks to all my family members. I am very grateful for all of the sacrifices that they have made and for supporting me in challenging time.

Sincere Regards,

Arpi Shah
Kingston University
2016

Abstract

Active magnetic bearings (AMBs) are used in many high speed machinery applications because of their advantages of no contact, no wear, no need for lubrications and ability to operate in high rotational speeds. AMBs represent an alternative solution to traditional mechanical bearing due to their contactless working principle. Touchdown bearings are needed in AMBs to prevent system damage under certain conditions such as sudden impact or sudden change of unbalance. In these conditions, rotor may make contact with touchdown bearings. AMBs may have the capability to accommodate sudden impact without contact though this will require novel design of control strategy for thrust and touchdown bearing. The purpose of this work is to provide platform for the robust control design research of flexible rotor-AMB touchdown systems. To this end research work concentrates on the design, construction and simulation of magnetic thrust and touchdown system.

The report begins with the identifications of flexible rotor AMB system configuration. In this content accurate rotor system model considering AMB, thrust and touchdown discs was obtained using FEM technique according to Timoshenko beam theory. Design of flexible rotor AMB system requires careful attention towards rotordynamic design aspect such as observability and controllability and it is important that actuator and sensor location are away from the nodal point. Identification of flexible rotor-AMB system model is achieved in a series of steps. Free-free undamped mode shapes were obtained in this work which predicts the dynamic behaviour of the flexible rotor. The plot of the free-free mode shapes and natural frequencies results have shown that the system is controllable and observable. Second, Campbell diagram was generated to see the effect of gyroscopic behaviour on the splitting of natural frequencies into forward and backword modes. Campbell diagram results showed satisfactory behaviour of flexible rotor.

The second goal of this work is to acquire technical design, modelling of electromechanical components and control unit. Magnetic actuator design specifications were obtained based on magnetic circuit analysis. Unigraphics software was used to carry out detail design and 3D modeling/assembly of electromechanical components. In this context purchase cost estimation was identified based on quotations. Purchase of rotor model components were made outside.

The third goal of a thesis work is to verify the flexible rotor system model using experimental test. Hammer used as a force transducer was used in the test as excitation of the system and accelerometer used to measure response of the system. The experimental result validates the FEM technique because it is in reasonably good agreement with simulation results. The experimental mode shape results showed rotor will perform well within design speed range.

Preface

The thesis is split into four main chapters

Chapter 1 Introduction

This chapter provides an overview of the basics of AMB theory, various configurations of a rotor-AMB test rig and the issues associated with rotor/touchdown magnetic bearing. The basic introduction is given here should allow non specialist in area to get the main purposes. Further, author present a systematic review of rotor touchdown contact behaviour in magnetic bearing system and previous research work related to impact. Author describes an overview of rotordynamics and the role of rotordynamic in the design of the AMB system by examining a number of research studies.

Chapter 2 Preliminary Design and Simulation of flexible rotor-magnetic thrust and radial bearing system

The author presents an iterative modelling process of the flexible rotor using finite element modelling technique. This chapter introduces a configuration of the rotor/touchdown thrust system. The current chapter also summarised the frequency response results and mode shape results obtained by using Ansys Workbench software. In addition, chapter describes the principle components of rotor AMB system and provides design specification for AMB system components such as coils, power amplifier, and sensor, rotor. At the end of this chapter, short descriptions of project cost estimations are given.

Chapter 3 Test rig experimental Validation

This chapter illustrates a laboratory experiment, undertaken at Kingston University Roehampton vale campus to determine the natural frequency and mode shape of the rotor. Modal testing technique known as hammer test was carried out and comparisons of both experimental and FEA results are investigated.

Chapter 4 Conclusions and future work

Here, main conclusions for this thesis are formulated and future work is discussed.

Nomenclature

Active magnetic bearings

A_a	Pole face area	m^2
B	Magnetic flux density in magnetic bearing coil	T
F	Force generated by one coil	N
$K_{\dot{C}}$	Current to force gain of magnetic bearing coil	N/A
K_x	Open loop stiffness of the AMB	N/m
N	Number of the coil turns	
μ_0	Permeability of free space	H/m
I_b, I_c	Bias and control current	A
s	Air gap	g
D	Diameter	mm
α	Pole angle	rad
V	Voltage to the AMB actuator coil	V
L	Coil inductance	H
I	Coil current	A

Rotordynamics

f	Natural frequency	rad/s
C	Damping matrix	Ns/m
C_1	Bearing damping	Ns/m , Nms
G	Gyroscopic matrix	Nms
I	Identity matrix	
K	Stiffness matrix	N/m , Nms

M, N	Global mass and inertia matrix	$\mathrm{K_g}$, $\mathrm{K_g}m^2$
$\dot{U}$	Velocity vector	m/s
$\ddot{U}$	Acceleration vector	m/s^2
R	External force vector	N
Ω	Rotational speed	rad/s
f_n	Natural Frequency	$\mathrm{H_z}$
w_n	Natural Frequency	rad/s

Abbreviations

AMB	Active magnetic bearing
ADC	Analogue to digital converter
FEA	Finite element analysis
ISO	International organisation for standardisation
PID	Proportional–integral–derivative
CAD	Computer aided design
CAE	Computer aided engineering
AC	Alternating current
RPM	Revolutions per minute
MIMO	Multiple input, Multiple output
API	American petroleum institute
FRF	Frequency response function
FFT	Fast fourier transform
DSA	Dynamic system analyser
RTI	Real time interface
PWM	Pulse width modulator
I/O	Input/output
D/O	Digital output

Table of Contents

List of Figures

List of Tables

CHAPTER 1

Introduction

The idea of levitating mechanical structure was well understood long time ago and goes back to Earnshaw [1] and Braunbek [2]. This concept has found many applications. The first rotor supported by an active magnetic bearing system (AMB) was developed by S2M in 1976. Figure 1 represents the latest version of the turbomachinery magnetic bearing system which is also used in many studies for research purposes [3]. Active magnetic bearing systems enable the rotor levitation without contact, wear, lubrication and provide users with accurate rotor vibration and position control. These elements make them suitable for high speed turbomachine applications. A number of research studies have been published that represent efficient, safe and reliable rotor-AMB system and so far significant improvement have been achieved in performance [4].

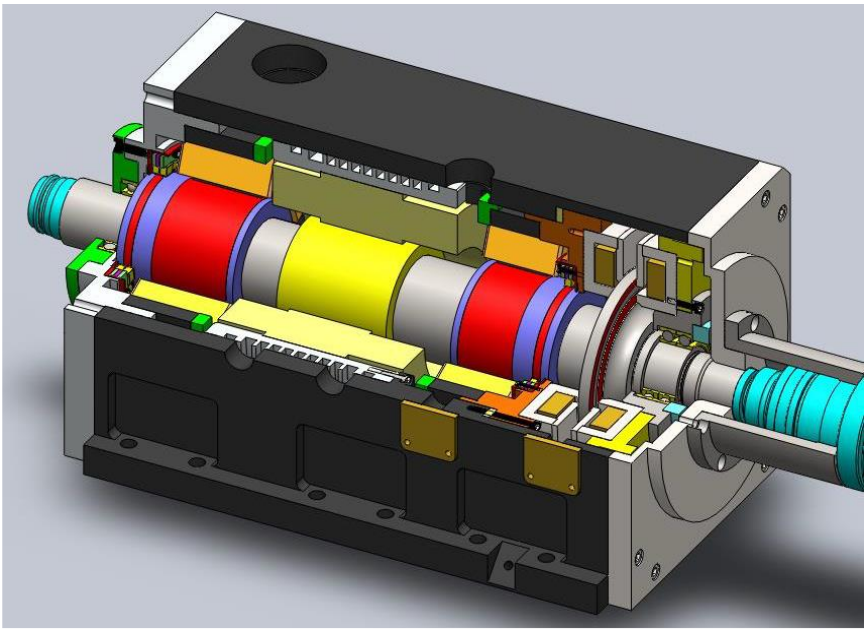

Figure: 1 modern version of the AMB system structure that shows radial, axial and touchdown discs [75]

1.1. Background on AMB System

In the rotating machinery, the use of magnetic bearings for rotor support is a recent innovative development. The major need for research in this area is towards 'reliability' because new applications are demanding safer and higher speed systems, and AMBs are expected to provide reasonable performance over its design life [5][6].

The active magnetic bearing is typically a complex interdisciplinary product which consists of mechanical parts, electrical parts and control systems, where the rotor and retainer bearing are mechanical parts, sensors and amplifiers are electrical parts [7].

Considering mechanical part, rotor is in the centre of the system surrounded by stationary electromagnets. Normally, for each radial bearing there are eight electromagnets placed 45° degree apart to the gravity axis [8]. These enable the actuator to lift shaft in any directions. However, few commercial applications may have different arrangements, where magnets can split into four different quadrants. Most AMB application systems are equipped with two radial actuators. Basic components and configuration of AMB and cross section of radial actuator is shown in figures 2 and 3 [9].

Taking electric parts, AMB controller read the signals from the radial displacement sensor and sends the signal to the power amplifier based on the difference between the sensor and a reference signal. Additional command signal is sent to the actuator so that it may bring back rotor on its original axes. When AMB is in operating condition, there are two types of load acting on rotor, dynamic load and static load. Mechanical static loading of the machine includes: machine elements of the system, rotor weight, etc., while dynamic loads may involve: external disturbance, impact force etc. Normally, bias current applied to support the static load, however if negative stiffness in magnetic bearing occurred, rotor moves from its original position and causes problem in the system. Therefore a control system must be used to bring back rotor to its own axis [10] [11].

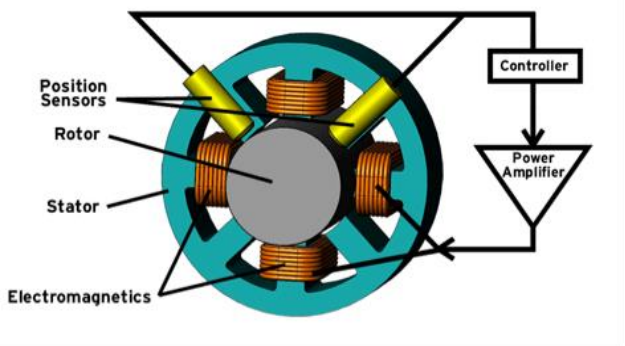

Figure 2: Basic components of AMB [76]

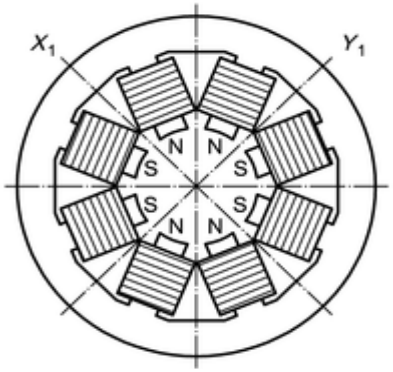

Figure 3 Configuration of radial actuator [9]

Typically, AMB systems have at least one axial actuator to withstand axial loading. Axial actuator consists of solid rotor discs placing between a pair of static actuator. It works similar to radial actuator but only withstands axial loading and cannot resist radial force [13].

Rotor stable levitation and position control would be possible with a set of radial and axial actuators; however, they are often driven by asynchronous motor for long term reliable operation. Figure 4 shows standard configurations of rotary AMB systems [14].

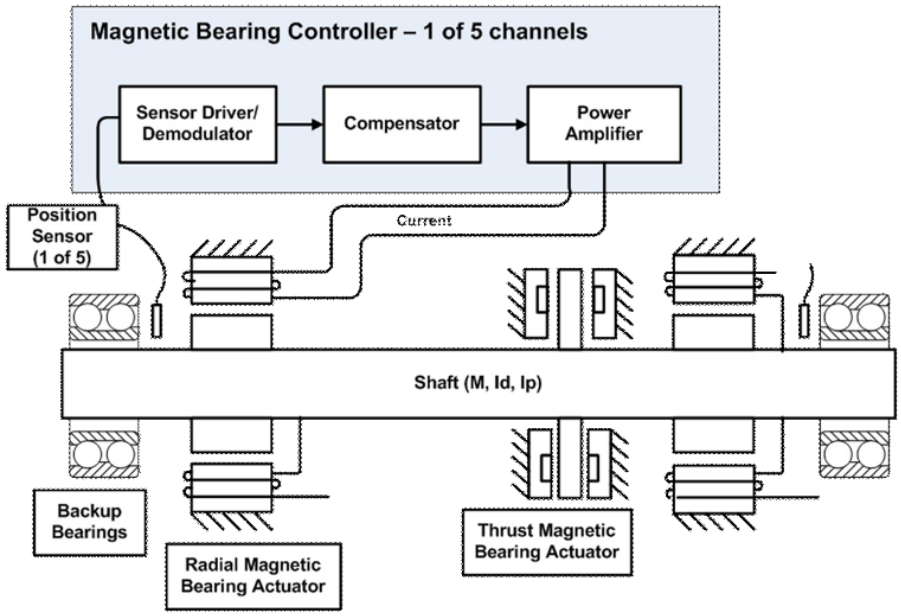

Figure 4: cross section of rotor supported AMB [6]

Rotor equipped with AMB has also back up bearing or safety bearing. Back up bearings provide rotor support in case of sudden loading or power failure of magnetic bearing.

Although, main application of the backup bearing is to make sure rotor does not lay on AMBs when the machine is switched off or when machine is in fully working condition. Figure 5 presents retainer bearing unit [6] [9].

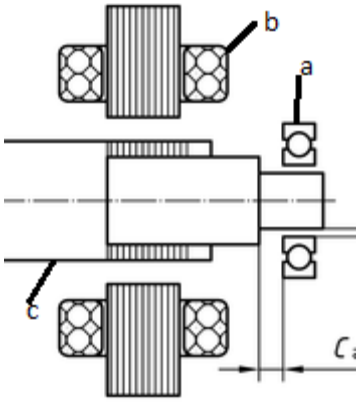

Figure 5: Back up bearing unit, [above, a=auxiliary bearing, b=AMB, c=rotor]

The rotor-AMB design with the motor drive enables contactless rotation between stationary and rotating parts. In addition, magnetic bearings when operated as actuator provides direct control of rotordynamics through feedback control method and provide longer system life [15]. Overall, their unique features have several advantages as below here.

- Magnetic bearings provide minimum friction losses, and longer operating life.
- Compared to conventional bearings, dynamic properties of AMB are easy to measure and change.
- Magnetic bearings not require lubrications therefore they have less operating and maintenance cost.
- Magnetic bearings provide high running speed, efficiency and prolonged machine life and it can be used in all kinds of environmental conditions.
- Under certain loading condition, high level static stiffness of AMBs provides precise control of the shaft centre [16].

Despite all of the advantages, AMBs have a limitations and disadvantages due to their design, material and physical constraints. Some of these limitations are:

- AMB actuator dynamic force capacity is frequency dependent based on equation $V = L\,I\,\omega$. Where V is the voltage, ω is required frequency and L is coil induction, I is the coil current. Therefore, if voltage is not enough to force the design current then dynamic load capacity will fall while increase in frequency.

- Magnetic bearings suffer from losses; mainly due to eddy currents that limit the Magnetic actuator bandwidth. During operations, for the AMB system to respond dynamic load, the controller must pass dynamic control flux through actuator poles. This control flux generates eddy currents which results in resistive losses.
- Materials used for AMB minimize the actuator load capacity as all materials have different saturation flux upper limits.
- Magnetic actuator cooling and winding insulation temperature are very important because copper losses produce the heat within the actuator assembly therefore the system needs enough cooling arrangement to remove heat.
- Magnetic bearing cost is much higher and expert knowledge requires for the design [6][18].

Because of their non-contact, lubrication free and adjustable dynamic characteristic the applications of AMB became much wider used during the past two decades. Their applications are not limited to high speed machinery, but AMBs are now found in other non-traditional applications where design and operations of compact devices are required to integrate mechatronic techniques. While new fields are constantly emerging this are not limited to mechanical industries but it also combine the electrical and computer science [18].

Magnetic bearings are widely used in gas turbine engines, where it needed to operate in an extreme environment. AMB can operate in high temperature environments and do not require oil. Kasarda [17] in his study gave an overview of magnetic bearing applications and advantages for the centrifugal compressors, rotary turbo machinery and machine tool spindles. One example is the NOVA natural gas pipeline, commissioned a 10,444 kW centrifugal compressor in 1985 which was integrated with AMB [19]. Alves and Alavi discussed that magnetic bearing compressor more efficient than conventional bearings. Later, similar reliability numbers were discussed by many magnetic bearing manufacturers for turbo applications [18].

Zmud reported that AMB can provide long operating life and able to provide very low friction losses [19]. AMBs are used in the flywheel storage system where energy losses need to be minimal. Mostly, an advanced monitoring system is integrated into magnetic bearing that can monitor the rotor position, vibration, current, temperature as well as unbalance responses.

The control action can change bearing design properties and allow stable performance. The application of magnetic bearing equipped with the rotor bearing system has seen in synchronous and vibration control [17][21], for vibration suppression and for active health monitoring of rotordynamic systems [42][43], magnetic bearings are applied in precision machine tool operation such as grinding, cutting because of their high level

performance in terms of high speed, low friction, high precision. AMBs are benefit having low stiffness in such application and achieve stable and longer machine life [21].

In high speed applications, AMBs are used to support the high speed rotor, here bearing properties such as damping can be varied during operation; therefore, it is necessary to cross these different critical speeds. AMB have advantages in such applications by avoiding different critical speeds using active method.

In many rotary machinery applications, AMB equipped with a flexible rotor and machines are operated above its first critical speed and this is a very critical mode as if it occurred within the sensor positions it may induce problems in control design. This problem can be solved with advance control action where it is necessary to include an accurate structural model of the rotor in control design. Prototype with an accurate prediction of rotor system dynamics is important to investigate control design. This can provide platform for many studies [25].

1.2. Rotordynamics

Rotordynamics is a part of engineering field that helps to study the dynamic behaviour of rotating shaft with an aim to find rotor vibration. It plays an important role in the designing of AMB system and controller. For industrial applications of a simple rotor bearing system, rotor dynamics are concerned with determining critical speeds, gyroscopic effect, instability, and unbalance response[8][3][25].

The books by Kramer, Child and Ishita provide to a reader valuable information for rotary machine design and analysis [62][63][64]. Plenty of research publications explained. rotordynamics analysis for both rigid rotor as well as a flexible rotor model. Studies have shown that for rigid rotor analysis, natural frequency values are much higher than the bandwidth of control system and can be controlled with PID. Flexible rotor provides much low eigenfrequenies. However, these frequencies can be affected by a controller; therefore a flexible rotor supported on AMB requires a careful observation of rotordynamics design aspects, electromagnetic and control design [25].

In a flexible rotor-AMB system, dynamics of bearing can bring nonlinear characteristics. A lot of research has been carried out on the non-linearity of the rotor bearing dynamics. These studies presented various calculation methods and techniques to obtain a nominal rotor model and dynamics of the system.

In 1998 Mohiuddin made a comparison of variety techniques for vibration analysis of rotor-AMB system [65]. At the start, he used finite element technique (FEA) for discrete approach, here rotor bearing system expressed by the equation of motions expressed by a set of ordinary differential equation for each node. The second method was a numerical method where the equation of motion was expressed by partial differential equations at each node. Further, he employed Lagrangian approach and modal reduction method. Goasch carried out modal testing and modal analysis where he included dynamics of foundation in the equation of motion via the recceptance technique [26]. However, results obtained from this study showed the inconsistency because analytical method is derived from incomplete measurement and with noise.

Finite element modelling methods have been largely used for flexible shaft/AMB dynamic modelling. Typically, FEA method is obtained by dividing geometry into a number of elements depending on geometry shape and these elements are connected to each other with nodes. Stephen and Roach used FEA technique for rotor bearing foundation system analysis [66]. They showed that using modal analysis, systematic approach it could be possible to measure frequency response function to incorporate the dynamic effect of support structure.

Vance in his studies used transfer matrix method and included comparisons of experimental results and computer predicted results for rotor bearing test setup [27]. In the majority of nonlinear dynamic studies which include different types of bearings, the gyroscopic effect and flexibility of the rotor part are ignored while obtaining the overall equation of motion are neglected. Jeffcott presented a very basic model, where he assumed that a rotor structure has no damping, a rotor is axially symmetric and has point mass. Later he extended his model by considering damping [29].

Kirk and Gunder presented steady-state and transient response of Jeffcott rotor with elastic bearings [28]. They ignored disc gyroscopic effect and rotor flexibility in the expression of the equation of motion, and presented design chart for with and without rotor supports. These studies state that due to gyroscopic effects the system matrix become asymmetric. Therefore, on the eigenvalue problem of the rotor bearing system, equation of motion are depended on undamped and damped gyroscopic system. Later, Nealson gave the global equation of motion for flexible shaft supported with journal bearing [29]. This equation was based on Tim's theory where gyroscopic effect and shear effect are taken into account; it was acquired from finite element matrices and used to indicate the general description about AMB system. The following equation of motion, which is based on Newton's second law of motion, describes the rotor-AMB system [30].

$$[\mathrm{M}+\mathrm{N}]\{\ddot{\mathrm{U}}\}+\mathrm{C}\{\dot{\mathrm{U}}\}+\mathrm{K}\{\mathrm{U}\}=\mathrm{R} \tag{1.1}$$

Where $[M]$ is the global translational inertia matrix for shaft, $[N]$ indicates the global rotatory inertia matrix, $[K]$ represents the shaft and bearing stiffness matrix and $[C]$ represents the generalized damping matrix that is due to bearings, where $[C] = [C_1] - \Omega[G]$ here $[G]$ is the shaft gyroscopic effect matrix. The matrix $[C_1]$ is a bearing damping, $\ddot{U} =$ Shaft acceleration, $\dot{U} =$ velocity and $U =$ displacement vector and Ω is the rotating speed for shaft, R represents the external excitation force [31].

1.2.1 Flexible rotor modelling and eigenvalues problem:

As mentioned earlier, vibration analysis of the rotor is used to find useful information on dynamic response of rotor. At the initial design of AMB-rotor system this analysis results can bring essential information for the dynamic behaviour of the system. Eigenvalues and eigenvector provide important data for mode shape and stability of a flexible shaft supported on bearing system. Free vibration of the system generally leads to eigenvalue problem and begin with deriving the natural frequency of the system under different conditions.

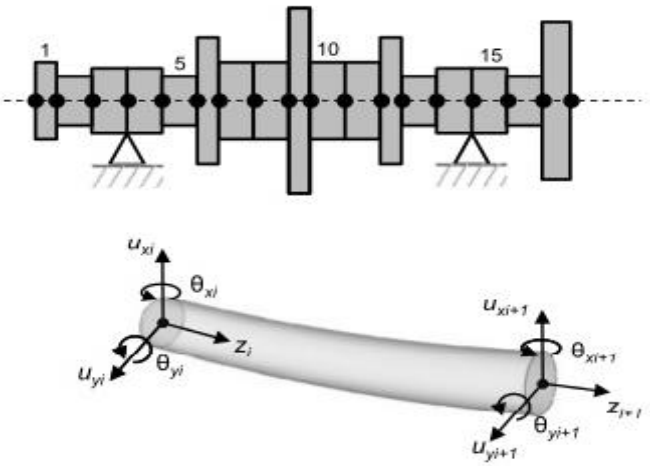

Figure: 6 example of rotor mesh and co-ordinate system of beam element [3]

For the eigenvalue problem, Equation 1.1 can represent in standard form using a similar method available in the reference [29]. $\{X\}$= state vector and it can be defined in the following form,

$$\{X\} = \left[\{\dot{U}\}^T \middle| \{U\}^T\right]^T \tag{1.2}$$

State vector $\{X\}$ is used to rewrite equation 1.1 and for free rotor condition equation 1.1 can be written as:

$$[M^*]\{\dot{X}\} + [C^*]\{X\} = \{0\} \tag{1.3}$$

Here,

$$[M^*]=\begin{bmatrix}[M]+[N] & 0\\ 0 & [I]\end{bmatrix}$$

$$[C^*]=\begin{bmatrix}[C] & [K]\\ -[I] & 0\end{bmatrix}$$

Here I is the identity matrix; the solution of equation 1.3 has the following form:

$$\{X\}(t)=e^{st}\{X_0\}(t) \tag{1.4}$$

And related eigenvalues can be represented as:

$$s[M^*]\{X_0\}+[C^*]\{X_0\}=\{0\} \tag{1.5}$$

$$[A^*]\{X_0\}=s\{X_0\} \tag{1.6}$$

Here $[M^*]$ is a non-singular,

$$[A^*]=-[M^*]^{-1}[C^*]=\begin{bmatrix}-([M]+[N])^{-1}[C] & -([M]+[N])^{-1}[K]\\ [I] & 0\end{bmatrix} \tag{1.7}$$

Here, the matrix $[C]$ is defined as $[C]=[C_1]-\Omega[G]$, Where, $[G]$is the gyroscopic matrix while the $[C_1]$ represents the bearing damping. The variable s in equation (1.5) is the system complex eigenvalues. These values are made of a real part and imaginary part "a" and "b" respectively and given by,

$$s=a\pm ib \tag{1.7}$$

Value "b" the represent natural frequency while "a" provide system stability information.

There are number of software codes available to perform modal analysis, and calculate dynamic responses of the rotor bearing system such as Ansys, Unigraphics, MSC, Marc. Mostly, Results obtained from this software codes are based on theoretical foundation for dynamic of rotor. However, software has limitation when it comes to complex dynamic analysis.

1.3. Configurations of AMBs

In this section, a short review of different AMB technology configurations is presented. Research studies have presented variety of AMB configuration that is small, simple, yet give desirable performance. Lee in his study developed a permanent magnet bias system that is capable to withstand any radial and axial load [30]. This design is a small and compact size AMB structurer. Jeng introduced AMTB (active magnetic thrust bearing) design and validated experimentally [67]. Haberman and Brunet gave description on the active magnetic system incorporate with radial and axial bearings. In this study, permanent magnets have negative stiffness which effect on the control performance [32].

Another hybrid type AMB incorporates a permanent magnet. This bearing has advantages of low cost, longer life, and lower power consumption. Eddy current losses have a great influence on the rotational power loss. Kim and Lee presented hybrid magnetic bearing that can minimize eddy current losses [12]. Although, using only permanent type of bearing it is not possible to gain stability in all degrees.

Horikawa and Silva present a new concept of one axis controlled magnetic bearing [68]. Experimental study concluded that rotor stable levitation and rotor fixed position can be possible with this type of magnetic bearing. A single cone shaped AMB are very useful as it generate force in radial and axial directions. However, its dynamic modelling and control is very complex because of their dynamics.

Hen developed integrated motor bearing using laminated cores and rotor [32]. This bearing uses Lorenz force for rotor levitation. Later Kim and Okado extended the study by proposing a new disc type integrating motor bearing [33]. In 2006 Kim introduced five degree control AMB that integrated radial and axial bearing unit and homo-polar type coil configuration to reduce eddy current effect [12]. To levitate homo polar AMB system Lorenz type axial force as well as the Maxwell type radial force used. This type of bearing has great benefits in high temperature applications.

1.4. Issues in the design of Magnetic Bearing

Non-linearity and uncertainties: The important issues need to deal with any dynamic system is internal non linearity and external uncertainties. Rotor-AMB systems are become unstable when operating in open loop and require a proper feedback control. Literature presents a control problem that deals with the balancing of a rotating shaft. However, although the rotor shaft is well balanced there are always uncertainties exist

in the system. Additionally, due to sudden changes in external and internal dynamic properties or system faults AMB systems enter in highly non-linear state [37].

Unbalance: Unbalance in the rotor due to uneven distribution of masses may also result rotor stator contact issue. When components rotate along its axis, rotor tries to move along the direction of the force which causes vibration in the system. Continuous rotor vibration will be transmitted to the bearing component and causes a fault in the system [39].

Sensor Failure: The operation of the AMB system is depends on the performance of the displacement sensors. Positional sensors measure the rotor position and from this information the magnitude and phase of corrective forces are produced. However, many failures such as signal distortions, damage in transmission line causes a fault in sensor. Failure in any of the sensor can cause problems in rotor dynamic behaviour, sometime rotor comes in contact with retainer bearing and induced instability problem[3][4][6].

Amplifier and coil failure: Instability of the AMB system can arise when amplifier or coil fail due to power cut or unexpected fault in the system. In all AMB system each of the coils can affect the flux in the entire air gap. Unexpected fault results unnecessary losses in one or more of the control axis and due to this it brings rotor contact problems. Excessive coil losses and contact phenomena can cause rotor bounces and rotor vibration resulting excessive damage in the system. In some cases it can destabilises the whole control system [41].

Due to these conditions, rotary machinery with magnetic bearing system is equipped with mechanical safety bearing/back up bearing to provide support in the event of overload condition or system faults. These bearings are usually ball bearing or simple retainer rings having a smaller clearance than the magnetic bearing clearance and it does not carry any load during normal operation.

1.5. Review on rotor/touchdown bearing contact study

In magnetic bearing system, a flexible rotor is levitated and controlled in five axes. Touchdown bearing is mostly equipped in such systems mainly to prevent rotor/magnetic bearing stator contact. Variety of operating conditions such as fault condition may be lead to transient or sustained contact between touchdown bearing and rotor. And these rotor/touchdown bearing subsequent interactions may lead to a range of stresses and impact forces. Consequently, these conditions cause damage of the safety bearings. In many applications, it may require to shut the whole system to avoid further damages [38].

In the event, when rotor comes into contact with retainer bearing, the design parameter of retainer bearing has a great influence on the dynamic response of the system. Ishi and Kirk [40], Ecker [70], Zeng [69], reveal that stiffness, damping, co-efficient of friction of retainer bearing design parameter have a significant effect on the rotor behaviour. Study undertaken by Xie [41] discussed the behaviour of clearance, support stiffness and damping on the steady state response of the rotor/touchdown system. They used a bifurcation diagram to study dynamic behaviour and recommended that touchdown bearing with lower clearance, stiffness and high support damping will give greatest rotor dynamic behaviour. Normally, retainer bearings are provided half of the clearance of active magnetic bearing. Cole [42] pointed out from his contact study that gap between touchdown bearing inner race and rotor has a significant effect on the nonlinear dynamic performance of touchdown system. It is good if touchdown inner race should be allowed to accelerate as fast as possible. Raju [44] did a similar study as Cole where he used brass bearing and presented important results. Different retainer bearings type gives different dynamic behaviour such as and Swanson work [71] shows different dynamic behaviour from the bushing and rolling type bearing. Wang and Noah[72] mentioned in their experiment that the system should be designed such that it can operate in the free-free eigenmodes of the rotor and presented an accurate model for the sleeve auxiliary bearing while rotor drop condition. Common to all above studies, it is important to remember that non-linear dynamic analysis is essential for rotor/AMB-retainer bearing system.

Number of research studies examined rotor-stator contact problem after AMB failure. However, there is limited work related rotor-stator contact while the magnetic bearing is still functioning. As stated earlier, a sudden increase of the rotor vibration or unusual operating condition leads to contact problem; this contact may be transient. If this interaction is not taken into account while designing of controller it could worsen the dynamic response of the rotor. However, with proper feedback control action and it is possible to recover rotor position and return to normal contactless operation. This could also increase the life of touchdown bearing and reduce contact forces. Research in this area has great potential in the field of nonlinear dynamics of a magnetic bearing system and may open new opportunities for various applications such as highly coupled rotor /AMB system in sea and air transports and medical application where it is not possible to shut down the whole system. An early perception of the rotor/touchdown dynamic is important while designing the rotor substructure system [11].

Number of rotor drop test studies has been carried out on a flexible rotor bearing system to investigate contact dynamics. These studies have revealed a variety of rotor/bearing contact modes like rub and bounce modes. In recent rotor-stator contact related research, experiment studies attempted to measure the contact

forces. This is a novel approach to control rotor when it contacts with touchdown bearings.

AMB systems are open loop unstable and it required a proper feedback control. The major studies have focused on the control side to remove or reduce rotor/touchdown bearing contact. Several papers have been published that applied various control strategies to ensure that the stable levitation is achieved. Siegwart [74] et al., Lei and Palazzol [46] used linear PID controller with an associated general notch filter for the applications where rotor/auxiliary bearing contact is induced. Burrows and Sahinkaya [73] implemented more advanced and powerful control strategies. These studies provide valuable insight for rotor stable, reliable operation above its first critical speed and structural rotor modal needs to be included directly in the control design process.

Various rigs were designed, modeled and characterized solely for control investigation. University of Virginia designed and built rotor-AMB test rig to simulate future energy storage system dynamics and to use it for future control investigation. However, this rig has suffered from modal uncertainty. Li and Lin [47] presented modelling of high speed rotor with active magnetic bearing. They described systematic behaviour approach for modelling of high speed rotor with magnetic bearing. Zhu and Knospe [48] presented modelling of non-laminated suspension system, however; research related to industrial applications has not seen reported. This is important for future research.

1.6. Objectives of the thesis

- ✓ To design, simulate and validate a general flexible rotor magnetic bearing rig that can operate at speeds above 10,000 rpm and includes active bearing, touchdown bearing and thrust bearing. This objective will undertake the following task
- ✓ To design and model shaft together with other component using Unigraphics, CAD software.
- ✓ To obtain rotor free vibration simulation test (FEA) and find natural frequencies and mode shapes under variable AMB, touchdown, thrust bearing, together with various discs.
- ✓ To determine an appropriate AMB location together with touchdown and thrust bearing location that could make stable rotor levitation over the speed range, perform iterative FEA simulation process and find an appropriate rotor-AMB rig configuration that meets design requirement.

- ✓ To undertake design calculation and design AMB to achieve required load capacity and threshold, estimate design parameters for axial bearing, back up bearing, sensor, amplifier, motor and control system.
- ✓ To produce required manufacturing design drawings for AMB assembly, axial bearing assembly, and shaft.
- ✓ To carry out an impact test experiment to validate proposed rotor bearing system model.

CHAPTER 2

Preliminary design and simulation of flexible rotor-magnetic thrust and radial bearing system

2.1 Test rig overview

To provide a platform for new research associated with rotor touchdown contact problems and to bring new facility in our university, a new test rig is designed. Once the rig will completely manufacture it can be used to test and develop number of touchdown control strategies with the objective to reduce the rotor touchdown problems. The rotor touchdown contact problem while AMBs are still functional is comparatively new concept and it is in the early stage of development [49].

The system built-in this thesis is a complex electromechanical product consists of electrical parts (including amplifier, data acquisition system) and mechanical parts (flexible rotor). The test rig comprises of 800mm long with 15mm diameter of flexible steel shaft supported by three radial bearing and two double acting thrust bearing. One of the radial bearing can be used as an exciter in order to provide controlled motion to the shaft. Besides this, system has three touchdown bearings to protect rotor in the event of touchdown and to give rotor support when AMB is not working. Three other discs are added to increase mass of the shaft. Because of the additional inertia the total weight of the rotor is 5.10kg. The analytical /experimental model of flexible rotor provide capability of running over second bending critical frequency within the speed range up to 10,000 rpm. Magnetic bearing disc diameter is 55-mm with maximum force capacity of 1035N. Radial bearing has eight poles oriented in the direction of each of the orthogonal radial co-ordinate at $\pm 45°$ to the vertical line. Touchdown bearing is an angular ball type bearing, having inside diameter 45mm and outside diameter 90mm.

Total ten eddy current sensors are decided to be used for the displacement measurement in x and y direction. Six sensors will be used to measure rotor radial displacement and four sensors will be used to measure rotor axial displacements.

System consists of brushless AC motor to drive the shaft. It is coupled via flexible coupling (represented in Figure 7). Selected motor can run at maximum speed up to 11,000 rpm and has rated power 5.6kw. Further, system consists of dSPACE system (flexible prototyping system) and power amplifier for control set up.

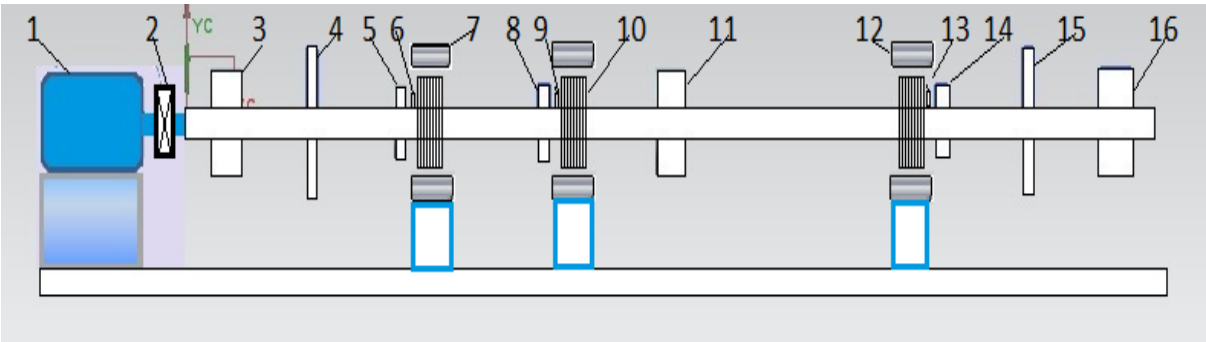

Figure: 7 Configuration of rotor magnetic thrust and touchdown bearing test rig discs (3, 16, 11-dummy Disks; 4, 15-thrust discs; 5, 8, 14-touchdown disks; 7, 10, 12-AMB discs; 6,13,9 –sensors location) all dimensions are in mm

Design of the test rig is a systematically approached and started with the design specification. During machine operations flexibility of the rotor may cause instability in the system; therefore the whole system configuration is produced after the rotor free vibration analysis.

In this chapter a brief overview of the typical design and construction methodology for flexible rotor AMB system is given. The objective achieved through the following tasks.

1. Design of the flexible rotor (including all bearing discs) using iterative finite element modeling technique. Here, in the beginning key requirement for flexible rotor design are formulated. After that, a flexible rotor AMB model at free conditions is represented based on the finite element modeling method, various simulation results were obtained and noted during analysis. Here, Ansys Workbench 9 was used for the dynamic analysis. During this task, a proposed configuration was designed such that it matches a real small rotary machine.
2. Design, description of the radial bearing, axial bearing, and rotor, stator assembly. Here, descriptions of the main active magnetic bearing components are present.
3. Control and hardware selection and purchase part list. In this part overview of selected dSPACE system and purchase costs are given.

2.2 Flexible Rotor design

Flexible rotor design in general is a difficult task as it often dictates a magnetic bearing physical configuration and contributes to the overall performance of the magnetic bearing system. It is difficult to modify system configuration once it is manufactured. Therefore, early prediction of rotor parameter and its effects need to analyse while the early design stage. Obtaining desire rotor-AMB configuration is an iterative optimisation process, where in the beginning critical map without damping and rotor mode shape generation speed is very useful [50].

In this thesis rotor design was led by some important key requirements. First, to ensure the rotor needed to display stable working within the frequency range of 10,000RPM. Second, to make sure when rotor is passing all critical speed modes it is away from sensor locations.

System modelling and analysis: Finite element modelling is done for the modelling of the rotor bearing system. Based on Tim's theory rotor was divided into a number of elements of the geometry. Each node has four degrees of freedom, two transitional and two rotational degrees of freedom. Figure 8 represents basic steps undertaken for modal analysis of free, flexible rotor-AMB. After many alterations rotor equipped with AMB discs, touchdown discs and middle discs was built in standstill condition; here axial disc dynamics were neglected for simplicity reason. For such rotor configuration, eigenvalues and eigenvector for the flexible mode was computed in Ansys Workbench finite element modal analysis application and frequency response and mode shape results was calculated. Figure 9 represents rotor-AMB mesh model and Figure 10 and Figure 11 represent modal analysis result for proposed configuration. A rotor diameter was 15mm and length 800mm while touchdown disc diameter 49.20mm magnetic bearing diameter 70.40 mm, and middle disc diameter 70.40 mm. A material specification for the shaft is shown in the following Table: 2.1.

Table 2.1: Material properties for the shaft

Description	Value	Unit
Length	800	Mm
Uniform shaft Diameter	15	Mm
Density	7850	Kg/m^3
Young's Modulus	210	GPa
Poisson's Ratio	0.283	
Total mass	5.10	Kg
Polar MOI	0.002376	Kgm^2
Maximum speed	10,000	Rpm

Next, iterative approach to improve configuration was carried out, where frequency response was measured by reducing shaft or discs diameter by 5 mm. at this stage,

discs were moved to different locations and FEA analysis for those configurations results was performed. The iterative rotordynamics procedure ends when the symmetric flexible rotor equipped with all discs, including axial discs configuration found within control bandwidth and when bending mode shape found away from the sensor, actuator axis locations and within critical speed range. Table 2 presents several modal analysis results from the complete optimisation process and Figure 12 shows rotor-AMB configuration that meets design requirements.

Eigenvalues are speed-dependent and it can be varied with stiffness value.[3] For the proposed configuration Campbell diagram is obtained where all damped frequencies are with respect to rotational speed. Stiffness value was taken based on mathematical calculation that is explained in the next section. Figure 13 represents a damped Campbell diagram.

Mode shape analysis summary:

The author describes a free vibration modal analysis of the rotor using Ansys finite element method, after the design stage mechanical layout of flexible rotor supported with AMB partially defined. However, this simulation does not include all subsystems that are another aspect of analysis. Chapter represents rotor mode shapes without PD controller for each bearing. For the results shown, first two modes are rigid body modes of the rotor while the next mode is flexural mode. First two modes are located away from the sensor and magnetic bearing location. The frequency of first mode is 46Hz, and, it can be seen that the second mode natural frequency is 141Hz which would again not cause any problem while control design according to design characteristic of rig. The higher modes results are not taken as investigation while analysing mode shapes.

Author obtained the Campbell diagram which was represented as a function of rotating speed. From Campbell diagram Figure 13 it can be read that when rotating speed equals zero, the rotor motion was ended in two planes and rotor has two natural frequencies which exactly match with two mode shapes. As soon as speed increases, two perpendicular planes separate which accepted as forward and backward mode. During operation, unbalance always excites only in forward modes which is based on first critical speed 46Hz.

Table 2.2: First three natural frequencies (bending mode) optimisation result for rotor-AMB configuration

No	Rotor Dia mm	Disc Dia mm	Touch down bearing dia	Magnatic bearing dia	Rotor length Mm	1st mode Hz	1 st mode RPM	2nd Mode	2nd Mode RPM	3rd Mode	3rd Mode RPM
1	30	80	49.20	70.40	800	135.39	8123.4	379.27	22756.19	716.8	43008
2	25	75	44.20	65.40	800	104.65	6279	296.79	17760	560.91	33600
3	20	70	39.20	60.40	800	75.485	4529.1	217.34	13020	411.38	24682.8
4	**15**	**65**	**34.20**	**55.40**	**800**	**48.565**	**2913.899**	**142.64**	**8558.4**	**271.44**	**16286.4**
5	10	60	29.20	50.40	800	24.908	1494.48	75.368	4522.08	144.03	8641.8

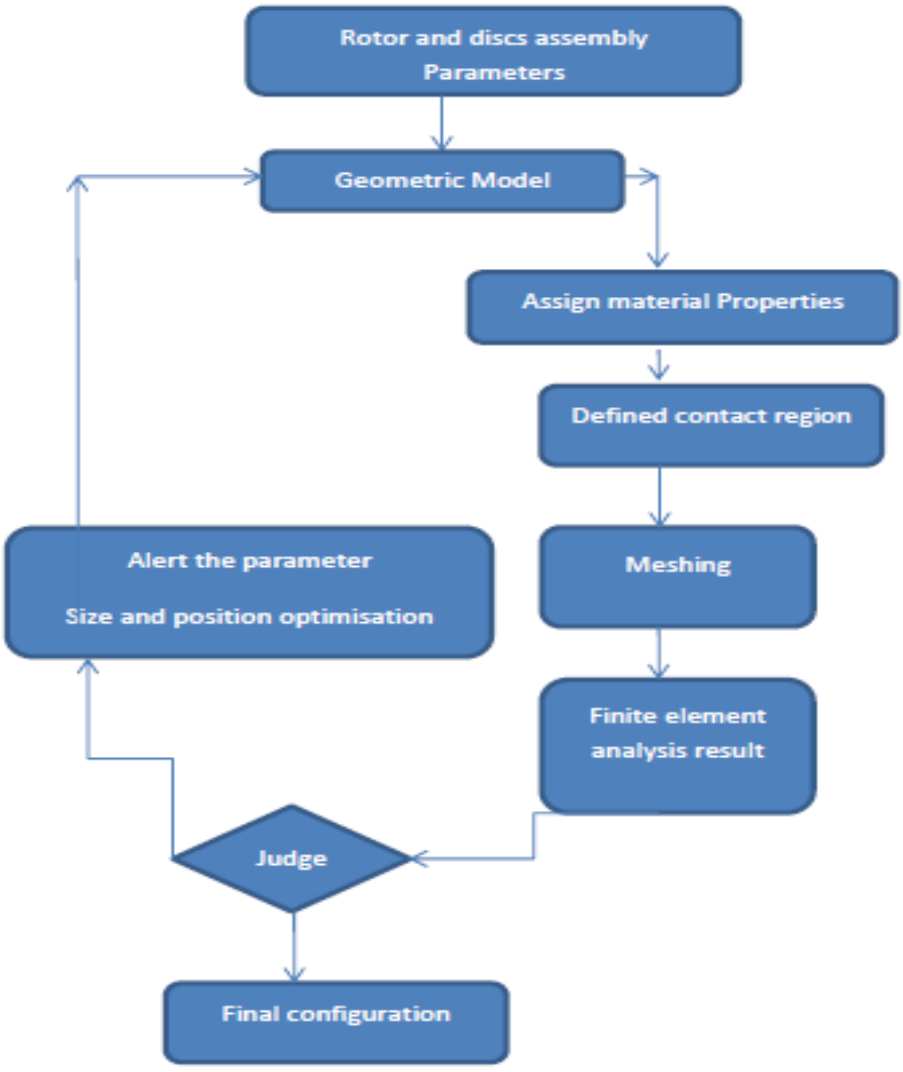

Figure 8: Flow chart of finite element modal analysis process steps undertaken in CAD/CAE software

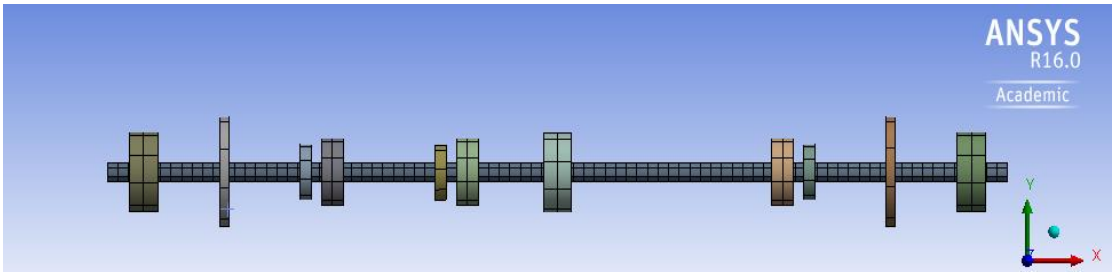

Figure 9: Finite element mesh model obtained in Ansys workbench16

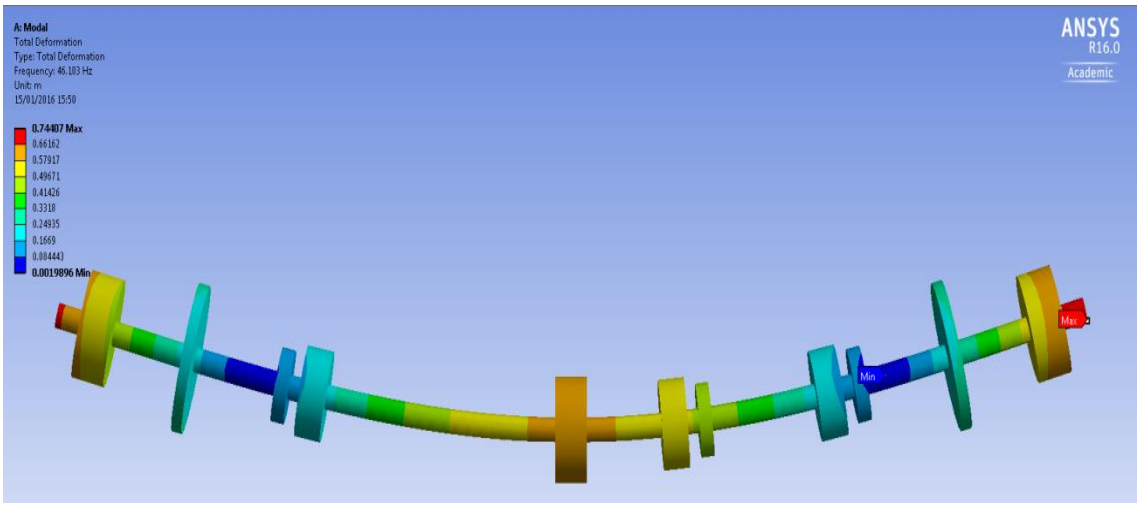

Figure 10: First mode natural frequency response at $\mathcal{F}_n = 46.2\mathrm{H_Z}$

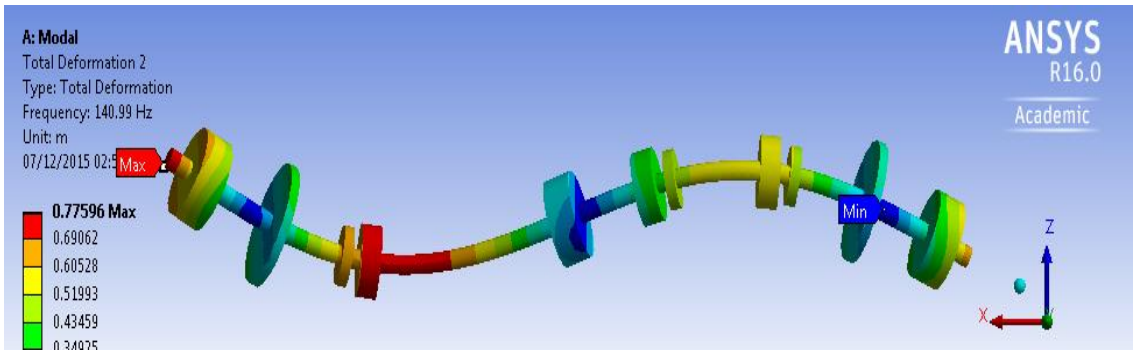

Figure 11: Second mode natural frequency response at $\mathcal{F}_\mathrm{n} = 140.9\mathrm{H_Z}$

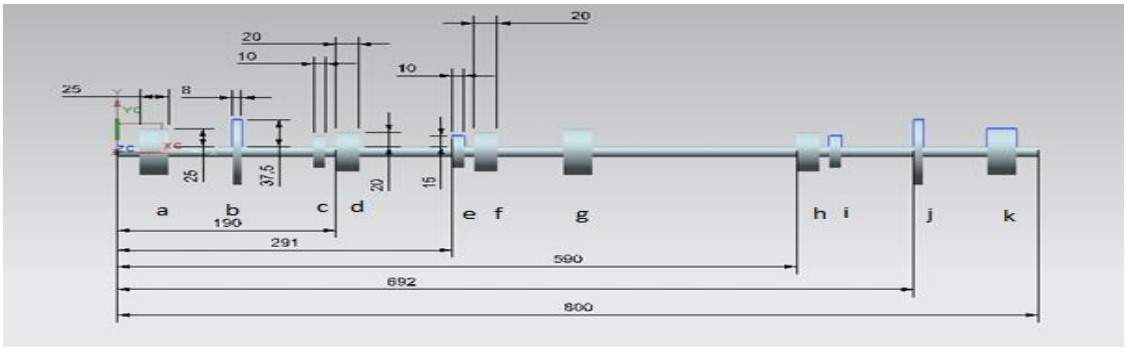

Figure 12: CAD model of rotor, discs (a,f,k-Dummy Disks, b,J-Thrust discs, c,e,i-Touchdown disks, d,g,k-AMB discs) all dimensions are in mm

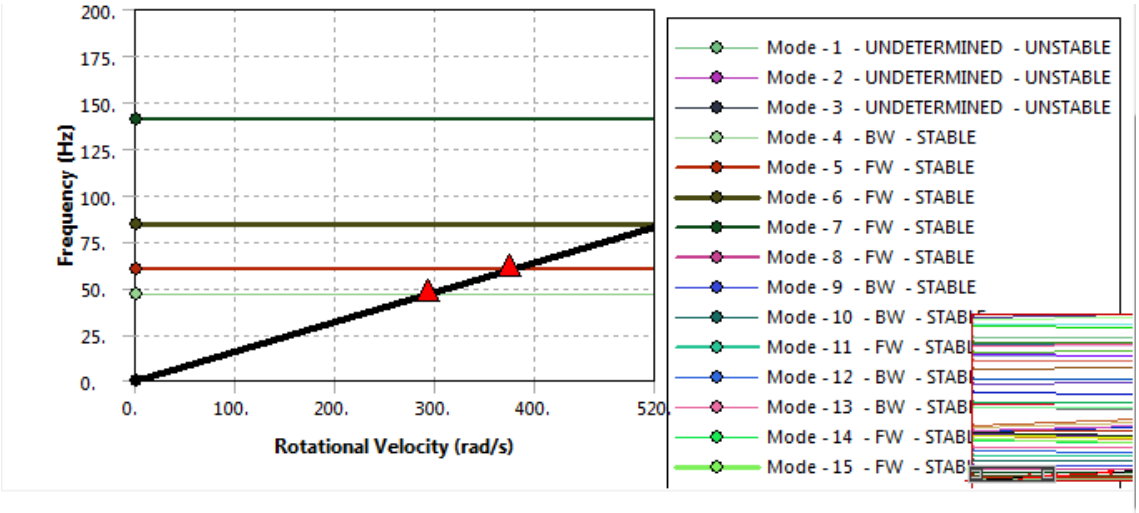

Mode	Whirl Direction	Mode Stability	Critical Speed	1. rad/s	1047. rad/s
4.	BW	STABLE	293.7 rad/s	46.858 Hz	46.45 Hz
5.	FW	STABLE	375.01 rad/s	59.654 Hz	59.74 Hz
6.	FW	STABLE	528.14 rad/s	84.08 Hz	84.032 Hz

Figure 13: Campbell diagram (x axis = rotational speed, y axis = damped natural Frequency)

2.3 Magnetic bearing rig components

The main design goal of the compact active magnetic bearings is to meet API617 design standard and take up radial as well as axial load while in operation. In the following section, detail design description of radial actuator and axial bearing and other main components of AMBs are presented. For profound design and modelling of magnetic bearing author referred to a book of Schweitzer and Maslen [3].

2.3.1 Radial bearing

Radial magnetic bearing is required in the system to lift the rotor and to minimize vibration which occurs due to unbalance forces [10]. For the proposed prototype; the radial bearings are made of eight electromagnets and arranged 90 degree as shown in Figure 14. The nominal radial gap of 0.5mm maintained between rotor and stator. The electromagnets are placed NS-SN-NS-SN directions around a cylindrical rotor part mounted on flexible shaft which to be levitated. With these heteropolar type radial bearing, it is possible to decoupled the axis and able to control vibrations equally in each of the axes. There are N number of insulated copper wire winding around each pole of the stator. The coils are inserted in core slots and pair of adjoining lamination coils are tied together in reverse series. The calculated laminations stock for actuator design is based on rotordynamic analysis, which is added to the rotor length.

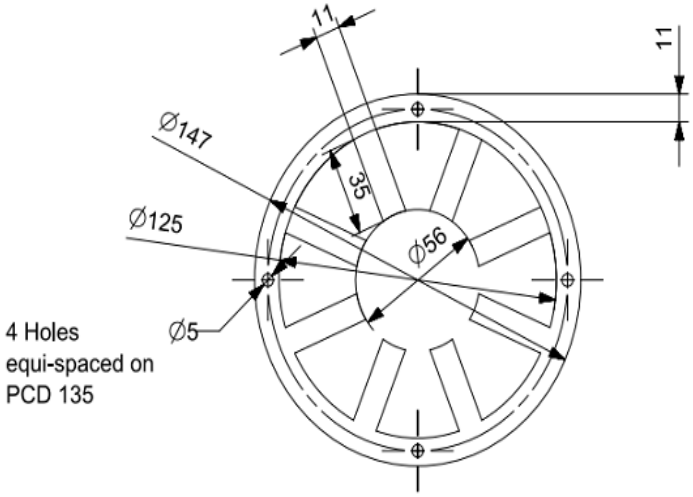

Figure: 14 Eight pole radial magnetic bearing

For the above model the feature of magnetic bearing is analysed via a magnetic circuit model. The model assumes negligible leakage and only small reluctance exists.

Maximum flux density in 0.5mm radial gap can be calculated as follows,

$$B_{max} = \frac{\mu_0 NI}{2C_g}$$

$$= \frac{4 \times \pi \times 10^{-7} \times 259 \times 4}{2 \times 0.0005}$$

$$= 1.3T$$

In terms of radial magnetic bearing magnet, electromagnetic force on the rotor is acquired from the current flowing through the coils and the air gap between the rotor and coil. Hence, effective force can be written as:

$$F_{max} = \frac{\mu_0 \, \mathrm{N}^2 \mathrm{A_a}}{4} \frac{\mathrm{I}^2}{\mathrm{s}^2} \quad (2.1)$$

Where μ_0 is the permeability of air ($\mu_0 = 4\pi \times 10^{-7}$ $[\frac{\mathrm{H}}{\mathrm{M}}]$), s = air gap, N is the number of the turns in coils and I is the current passing in the coil, $\mathrm{A_a}$ is the projected pole area [15].

And force produced by particular geometry is,

$$F_{max} = \frac{{B_{\max}}^2 \mathrm{C_g}}{\mu_0} \quad (2.1a)$$

$$= \frac{1.3 \times 1.3 \times 0.0005}{4\pi \times 10^{-7}}$$

$$= 1035N$$

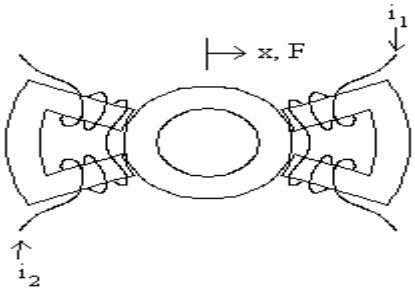

Figure: 15 Magnetic bearing force generation (one axis) [52]

In general, electromagnetic coils are placed in pair and the electromagnetic forces are pulled in opposite axis. The net force $\mathrm{F_x}$ is the difference between two forces in positive and negative directions.

Therefore force along x axis $\mathrm{F_x} = \mathrm{f1} - \mathrm{f2} = \mathrm{K_m} \left[\frac{{\mathrm{I_1}}^2}{(\mathrm{s}-\mathrm{x})^2} - \frac{{\mathrm{I_2}}^2}{(\mathrm{s}+\mathrm{x})^2}\right]$ (2.2)

$$\text{Here } K_m = \frac{1}{4}\mu_0 N^2 A_a$$

Nominal gap is s; force can define by deviation x, actuator current is I_1 and I_2

Force and current relationship is quadratic. Using perturbation methods equation may be linearized at the operating point and magnetic force equation for one axis can be written as follows,

$$f = K_x x + K_c I_c \tag{2.3}$$

Here, I_c is the control current and K_x and K_c are the open loop bearing stiffness and current coefficient, this can be calculated analytically and it is possible to find experimentally. According to ref [12] magnetic bearing current coefficient and stiffness can be written as

$$K_x = 4k\frac{i_0}{{s_0}^2} \tag{2.4}$$

$$\text{And} \qquad K_c = 4k\frac{i_0}{{s_0}^3} \tag{2.5}$$

Where k= magnetic bearing constant

Nominal design specifications are taken to calculate the force in active magnetic bearing that is shown in Table 2.3. Detail calculations are presented in appendix A.

Table 2.3: Selected design parameters for AMB

Description	Symbol	Value	Unit
Internal diameter	Ø	57	mm
External diameter	Ø	147	mm
Max Force	F_{nimax}	1035	N
Inner Diameter	D_i	56	mm
Air gap	C_g	0.5	mm
Flux density	B_{max}	1.3	Telsa
Permeability of free space	μ_0	$4\pi * 10^{-7}$	H/m
Pole angle	A	22.5	degree
Rotor mass	m_r	5.1	Kg
Maximum speed	Ω_{max}	10,000	rpm
Maximum current	I_{max}	4	A
Maximum voltage	V_{max}	15	V

Calculated control coefficient and stiffness are:

$$K_x = 221\,{}^{N}/_{m}$$

$$\text{And} \quad K_c = 53\,{}^{N}/_{A}$$

2.3.2 Axial bearing design

To take up any axial load when the rotor is moving with motor axial bearings are required in the rig. An axial bearing is made of two pieces and each has an electromagnet actuator. Axial disc is provided between these two parts which is going to shrink fit on the rotating shaft. Thrust discs are made a little thicker to avoid the possibility of flux entering into opposite pole [51]. Axial bearing has a capacity to generate forces in both directions. Further, it is designed to take higher load capacity in one direction while the rest is in the other direction. Figure 16 shows the arrangement of typical two axes axial AMB for this system where all parameters are involved in the design.

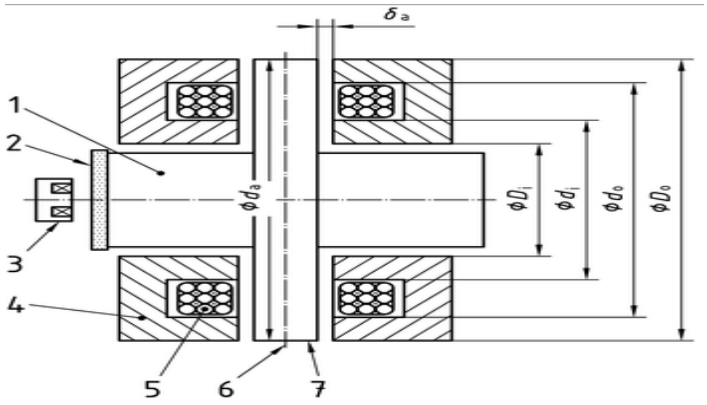

Figure 16: Axial magnetic bearing arrangement [3]

Detail design calculation is carried out using the equations presented in reference 54 and presented in appendix B. Initial specifications are used to design axial bearing which is shown in Table 2.4.

Table 2.4: Selected design specifications for axial AMB

Description	Symbol	Value	Unit
Internal diameter	$\emptyset d_i$	45	mm
External diameter	$\emptyset D_o$	90	mm
Max Force	F_{max}	110	N
Air gap	C_g	0.75	mm
Flux density	B_{max}	0.8	Telsa
Permeability of free space	μ_0	$4\pi * 10^{-7}$	H/m
Amplifier current	i_{max}	4	A
Maximum voltage	V_{max}	15	V
Number of turns	N	259	Turn

2.3.3 Touchdown bearing

There are three touchdown bearings, which are placed next to the magnetic bearing. These bearings are used to protect the magnetic bearing when rotor becomes unstable. The clearance of the touchdown bearing is smaller than magnetic bearing clearance; therefore shaft can freely rotate axially through the ball bearing in all conditions.

The touchdown bearing is consists of, touchdown discs, Angular contact ball bearing and cover. Double row angular contact ball bearing is the design and manufacture of SKF Company according to given design load requirement, rotational speed and environment condition rotor. This bearing has the capability to provide high radial and axial capacity and quiet operation. The ball bearing uses two single raw back to back angular contact ball bearings in one place. Inner diameter of the ball bearing is Ø45 mm and OD bore is Ø90 mm and width of the bearing is Ø35mm. The ball bearing is assembled with the touchdown disc, which is mounted on the shaft using cone clamping element. The touchdown bearing cover is screwed to the magnetic actuator bearing housing. (Shown in Figure 17)

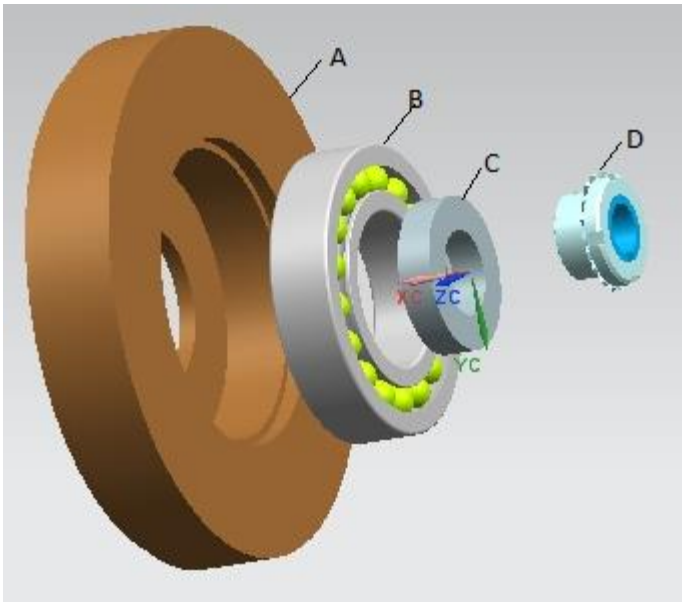

Figure: 17 Touchdown bearing assembly (A=Touchdown housing, B= Ball bearing, C=Touchdown disc, D= coupling element)

2.3.4 Rotor

Assembly of the rotor is consists of mainly rotor shaft and rotor core. Rotor shaft is made of steel as it has higher fatigue resistance compared to other material. Rotor

shaft specifications are given in Table 2.1. Rotor core is assembled separately with staking lamination coil with the required length. The end of the rotor core rig is inserted and screwed together using a long machine screw. Finally, the rotor shaft can be slowly inserted into the rotor assembly. Cone clamping elements from 'RINGSPANN' are selected to provide connection between rotor and shaft. The rotor assembly arrangement represented in Figure 18.

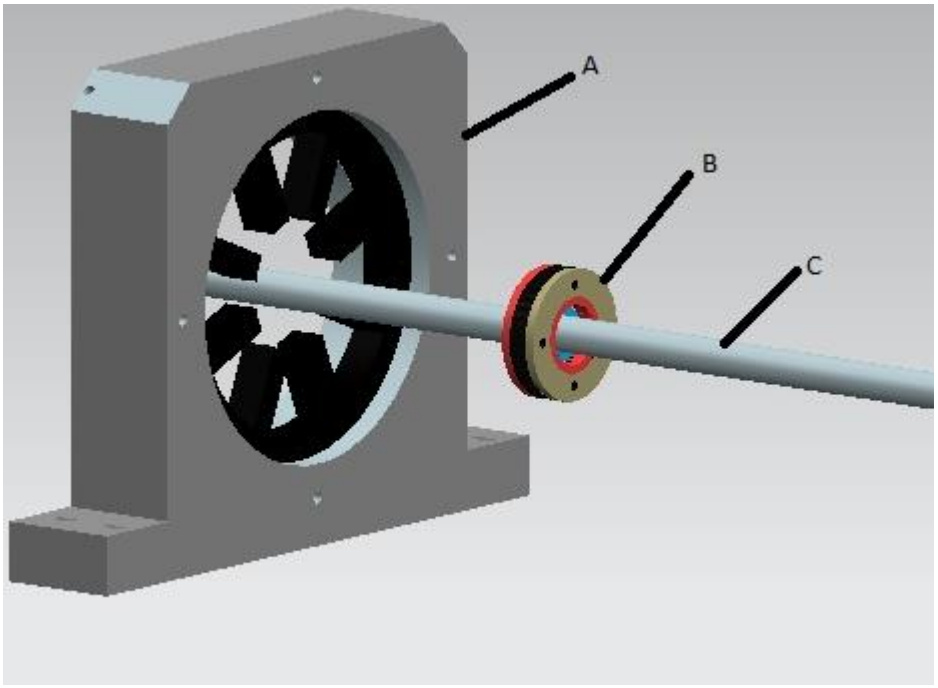

Figure: 18 Rotor magnetic bearing assembly (A= magnetic bearing housing, B=Rotor (with lamination, cone clamping, rotor core), and C=Shaft)

2.4 Control hardware selection and purchase parts list

Because of instability problems in magnetic bearing, this rig is required to incorporate closed loop controller, eddy current sensor, data acquisition, and power amplifiers [49]. Some of the control hardware parts are described in the following section.

2.4.1 Eddy –current sensor

As mentioned earlier in chapter 1, feedback loop are required to stabilize the AMB system. System uses a position displacement sensor to measure the rotor shaft displacement. The main requirements of a positional sensor are: first, they should be operating non- contact with a target, second, their frequency range need to be higher

than the power amplifier or magnetic bearing third, sensor tip material should be similar to the shaft material.

There are different types of non- contact position sensors are available that are used for magnetic bearing such as optical probe, laser probe, hole effect probe, eddy current probe. However; eddy current sensors are most widely used for magnetic levitation. Eddy current sensors work with magnetic field. They are made of the probe tip, which has two coils. Driver generates high frequency alerting current produced at the end of the probe tip. This brings magnetic field fluctuation and creates small eddy current in the target. The eddy current in the target creates its own magnetic field and interact with probe tip this causes a change in sensor coil inductance and produce voltage. The interactions are relied on the difference between probe tip and target. Therefore, the selected eddy current probe tip diameter is three times smaller than the shaft diameter.

Eddy current sensors measured the position of rotor shaft and provide position feedback to the controller. With the very minimum phase shift these sensors can provide frequency response. Further, they produced an opposite magnetic field and minimize inductance in the coil which helps for stable levitation of the rotor. However, eddy current probe with an actuator can cause an instability problem if rotor has not suitable characteristics. The sensor position at vibration node may lead to the poor performance. Eddy current sensors worked in a pair and the pair of Sensors is arranged $\pm 45^{\circ}$ to the vertical line. Total ten eddy current sensors are provided in the construction of the system. Where, set of two sensors (total six) are installed for each radial bearing to measure displacement in x and y directions and to satisfy collection condition. One sensor is installed on each thrust disc for axial measurement. Further, two pair of sensor are provided at the far end of the rotor. Eddy current sensors are part of the housing for AMBs and positioned as near as possible to magnetic bearing.

Output from the pair of the sensors is added to calculate position of the shaft with respect to the axis. The Figure 7 shows sensor arrangement near magnetic bearing.

2.4.2 Power amplifier

Servo power amplifier is used to drive current to the coils and to drive induction load of AMB coil. There are in total 14 of Copley Control Inc ('Xenus' model) micro digital servo control amplifier selected, where two of them for each radial bearing in x and y direction and one required for each axial bearing.

Selected 'Xenus' amplifier model uses PWM velocity/ torque command interface for power amplification and employ digital feedback to run in voltage mode and current

mode. Generally, servo amplifier keeps the shaft centre by Pulse width modulation to compare the signal with input values and provide power adjustment in magnetic coil.

Servo amplifier PWM output stage employs a transistor to produce positive and negative coil current from the single polarity power supply. These transistors are worked as switches. When transistors are off voltage is zero and no current flows through coils and when the transistor is fully on the voltage is above threshold voltage and represent current flow in the positive or negative direction. Therefore, resulting power dissipation is minimal [3].

Technical specification of the power amplifier is shown in the Table 2.5. Selected amplifier response can be measured with doing experiments where system analyser will used to generate sine wave and to get the current generated in the AMBs. However, experiment response is not part of the thesis.

Table 2.5: Technical specifications for power amplifier

Amplifier type	Digital servo type
Max Output current	6A
Continuous current	3A
Peak power	0.33 K_w
Voltage	14 ~ 55 V_{dc}

The main drawbacks of the power amplifier are significant noise as the current passing though the coil has ripple noise at the switching frequency. This noise can flow out to other electric system and causes the problem in the system. The close loop bandwidth of control loop causes the problem of noise. Hence, additional anti- aliasing low pass filtering of the calculated signal is necessary for filtering of coil current and rotor position.

Generally when anti-alising analog filter is implemented, high frequency noise removed before A/D conversation. The sampling of high voltage positional signal can be obtained in A/D converter and treated by digital signal processor. Since, digital signal process happens after A/D converter it removes noise occurred during operation. The command signal generated from digital signal proceed to the PWM

(pulse width modulator), which generate a series of constant voltage or current pulses to the power amplifier [3].

2.4.3 Data Acquisition System

dSPACE hardware/software system Inc name as “MicroLabBox” is decided to be used for control of the system. This system has a real time interface (RTI) that captures real time data and graphical interface to connect variable to data acquisition for real time display. Control kit MicroLabBox consists of DS1202 Dual Core 2 GHz processor board and DS1302 I/O board, top panel and various convertor channels. The analog input has sixteen of 16bit channels that operate with $1\mu s$ sampling time. Furthermore, analog input has additional eight 14bit channels with free running mode. Beside this, controller board has 48 bidirectional D/O channel. Moreover, system hardware includes another feature such as electric motor I/O functionality, sensor supply, and encoder interface.

The operating system processor operates with Matalab/Simulink environment. Simulink Library has all features to create and save model diagram, modify the initial specifications and export to other file. Simulink real time interface allowed to convert model base diagram to c code; this code, then downloaded to the processor and show real time simulation. Simulink hardware software system controls all variables without any interruption and allows changing system signal and experimental data in real time and automatically play simulation. It has the capability to run in free mode, trigger mode, recording data and saved collected data to matalab workspace [11].

2.5 Cost Estimations

Cost estimation is a process to know about how you will spend money. The procedure for obtaining the required quotations took one months starting with contacting three different suppliers and with the specification being sent to supplier. To get an overview of the project cost, the list of important purchase parts and associated costs can be made in Excel sheet. Table 2.5

Table 2.6 purchase part cost estimation in pound(£)

PURCHASE PARTS	QTY	Price	cost (Exluding VAT)
POWER AMPLIFIER	14	215	3010
MOTOR	1	75	75
SENSORS	10	226.62	2266.2
CONE CLAMPING ELEMENT	6	9.5	57
CONE CLAMPING ELEMENT	3	12	36
Microlab box	1	9,000	9000
AMB	3	500	1500
shaft + discs	1+8	426	426
Ball Bearing	3	30	90
			16460.2

2.6 Summary

In this chapter design, modelling, and simulation of a prototype five axes magnetic suspension system supported by the flexible shaft is presented. Finite element modal analysis is very important to give a quick imagine about how the system will perform. Iterative process of free-free modal analysis using finite element method is employed to test the rotordynamic behaviour of the flexible-AMB system and provides clear understanding of the frequency response. For the designed speed range, system showed stable operation. Further test result of model with gyroscopic effect also obtained, plotting its Campbell diagram.

Later, considering all the system components, overall system model and purchase cost estimation has been obtained. Cost estimation has given insight into how long and how much it will take to build the system.

CHAPTER 3

Test rig experimental modal analysis

This chapter discusses an experimental modal analysis technique known as hammer test, which is used to find natural frequency and mode shapes for the rotating shaft model created in chapter 2, comparison between experimental test results and the FE model simulation results are also discussed.

3.1 Experimental modal testing overview

Experimental modal testing more often refers to 'frequency response function method', which uses physical test to measure both input excitation and output response of the structure [54].

Experimental modal testing is widely used in research and industry to extract the modal model properties such as eigenfrequencies, mode shapes and damping. It determines the dynamic characteristic of a system. Data obtained from the modal testing are often used to compare the simulation technique in order to improve the efficiency of the system structure [53]. Modal test experiment can represent in three steps:

1. Preparation of test set up,
2. Data acquisition and
3. Modal characteristics identification.

The central idea of the experimental modal test is to get the FRF (frequency response function) of the structure. In most cases, during the test set up stage response points are marked and either impact hammer or shaker is selected to excite the system structure. These FRF measurements are recorded in dynamic signal acquisition analysis software/ multichannel FFT (fast fourier transform) analyser software. Software's are integrated with the intelligent wizards that provide systematic procedure to obtain the FRF data. Obtained FRF data can be synthesized in the software to find modal characteristics of the test structure [55].

3.1.1 Mobility measurement

Generally, three types of FRFs are obtained with varying vibration responses: acceleration FRF that corresponds to acceleration, mobility and compliance FRF which

corresponds to displacement and velocity. In this experimental work, FRFs were measured with acceleration because an accelerometer is the most appropriate motion transducer. The equation of the motion can be written in following form:

$$\frac{d^2x}{dt} + 2\zeta\frac{dx}{dt} + {\omega_0}^2 x = \frac{{\omega_0}^2 F}{k} \tag{3.1}$$

Where ζ is the damping ratio, ω_0 is the natural frequency, k is the stiffness and F is the external force

Transmissibility function can be represented in the following form:

$$H(\omega) = \frac{[\ddot{x}(\omega)]}{[F(\omega)]} = \left[\frac{1}{k}\right]\left[\frac{-\omega^2{\omega_0}^2}{{\omega_0}^2 - \omega^2 + j(2\zeta\omega\omega_0)}\right] \tag{3.2}$$

Magnitude of this function can be derived as:

$$H(\omega) = \left|\frac{\ddot{x}(\omega)}{F(\omega)}\right| = \left[\frac{1}{m}\right]\left[\frac{-\omega^2}{\sqrt{({\omega_0}^2 - \omega^2)^2 + j(2\zeta\omega\omega_0)^2}}\right] \tag{3.3}$$

And the phase can be written in following form:

$$\alpha = \pi - \arctan\left[\frac{2\zeta\omega_0}{{\omega_0}^2 - \omega^2}\right] \tag{3.4}$$

3.1.2 Coherence function

In impact testing, the hammer is hit at each point several times to get more accurate results. Thus, coherence function is important in making a good judgment of whether the set of measurements is accurate enough. Coherence function can be represents as:

$$C_{xy} = \frac{|D_{xy}|^2}{D_{xx}D_{yy}} \tag{3.5}$$

Here, D_{xy} is the Fourier transform of the cross-correlation function between x and y. D_{yy} and D_{xx} is the auto spectral density of x and y.

Preferably, recorded impact measurement responses of each hit the same, therefore, coherence graph should show a value of 1. However, in real test incoherence is always exists in impact test and cannot be avoided. Sometimes coherence function graph shows several notches, this are because of the poor signal to noise ratio although it does not require special attention. In general, coherence function shows good results if its value is higher than 0.95 at resonances.

3.1.3 Excitation

Mostly, a structure should have adequate magnitude of forced response amplitude and useful frequency range of the interest while excited. There are two different types of excitation methods most widely applied on the rotating structure: either hammer/impact test or shaker test.

For hammer test/impact test, hammer is utilized to generate excitation signal. Hammer has a force sensor at its tip, which measures the input force applied to the test structure, these force information believe to be equal and opposite to that felt by the test structure [56]. The head of hammers is made of stainless steel and hammer tips available in variety of the materials such as rubber and plastic. Selections of the hammer tip provide a control on the frequency spectrum of the test structure. The main benefits of hammer test are that it is fast and less expensive. However, it is difficult to get consistent hammer hit during tests. Further, careful attention is required towards hammer impact on the structure as it may cause problem in signal processing. Figure 19(a) shows hammer excitation used in this test.

3.1.4 Accelerometer

Typically, accelerometers are used in modal testing to measure the response acceleration. Based on different types, they can measure accelerations either allows one direction or three perpendicular directions at the same time [58].

In modal analysis, mass, sensitivity and frequency responses are taken into consideration for selection of appropriate accelerometer. Lightweight, compact accelerometers should be selected so it cannot effect on structural modes. There are many ways to mount an accelerometer on the test surface; among them adhesive was the only available choice in the lab for this test. Adhesive is the fast, easy and quick way of attaching accelerometer. However, if the coating is applied too thick it may influence on the quality of the measurement data. Accelerometer information is transferred to the FFT analyser software and this software provides measurement data and signal processing. Figure 19 (b) shows the accelerometer used in the impact testing [59].

Figure: 19, (a) Hammer

Figure: 19 (b) Accelerometer

Table: 3.1a Hammer specifications

Performance	English (Imperial)
Sensitivity	(±15%) 10 mV/lbf (2.25 mV/N)
Measurement Range	±500 lbf pk (±2224 N pk)
Hammer Mass	0.34 lb (0.16 kg)
Head diameter	0.6inch
Mounting	Adhesive

Table: 3.1b Accelerometer specifications

Performance	English (Imperial)
Sensitivity	(±10%) 100 mV/g (10.2 mV/(m/s²))
Measurement Range	±50 g pk (±490 m/s² pk)
Broadband Resolution	0.00015 g rms (0.0015 m/s² rm
Frequency Range	(±5%) 0.5 to 3000 Hz
Mounting	Adhesive

3.1.5 Dynamic signal analysers (DSA)

Analysis of vibration signals can be obtained using a data acquisition system called 'dynamic signal analyser'. In old days dynamic signal analysers used analogue tracking filter to measure FRF data. In recent trends, it uses digital technology to record frequency and to post process the measured data.

DSA comprises different electrical modules for advanced modal analysis, hammer testing and MIMO (multiple input multiple output) testing. Mostly, signal analyzers hardware connects with the PC or laptop through USB and the integrated software displays a necessary result on the PC screen. Data acquisition module of DSA has strong capabilities to compute real time FFT and time history data [60].

3.2 Experimental modal analysis

3.2.1 Overview

In order to validate the results of FEA method, an experimental measurement test was carried out to acquire frequency response data of mechanical test rig model. Considering the light weight of the structure in this experiment hammer was used for excitation system and one accelerometer was used for response measure. National Instruments dynamic Analyzer Software called 'SO analyser' which was preloaded in the PC was used for data collection and analysis. The properties of the shaft are shown in Table 2.1.

In practice, there are two ways to take this test either to rove the hammer or accelerometer. Either way it gives the same results. In this experiment test, hammer was roved because repositioning accelerometer could be time consuming and because of circular shape of the shaft it was difficult to mount accelerometer.

3.2.2 Experiment set up

Experiment set up is shown in Figure 20. The experiment was done in Learjet lab at Kingston University Roehampton Vale campus. As discussed before, a study of the free vibration will be helpful in understanding the dynamic behaviour of the rig therefore in this test free- free boundary conditions was realized on the new rig. Test rig was suspended using bungee cord allowing desired free motion for the modal test. Accelerometer (model 333B32, sensitivity 97.2 and 98.6 mv/g) was fixed with shaft using adhesive at non driving end of shaft. There were total two channels connected in the hardware where input channel connected to the hammer and output channel connected to the accelerometer. Before taking measurement, it is necessary to check all electrical connection including the connection between National Instruments acquisition hardware and PC. Amplifier was switched on before taking measurement and voltage knob was set into anticlockwise.

3.2.3 Experimental procedure

1. In the beginning of the process, there were total 10 points marked symmetric along the y axis of the shaft. The position of the each point was obtained from the nodes of the FEM model. These points were used as reference for data acquisition.
2. Configuration of shaft was constructed as a straight line in 'SO analyser' geometry wizard. Measurement parameters such as sampling frequency, block size, manual arm mode were set in the SO analyzer software.
3. Channel 1 was defined as excitation and channel 2 was defined as accelerometer and their units were defined simultaneously in the software. Measurement frequency range was set between 0 to 280Hz .
4. Hammer was hit at each point three times and the response was measured by accelerometer. It is important to mention that if the software shows double hit, the reading need to take again because double hit may cause inconsistent frequency spectrum.
5. Fast Fourier Transform (FFT) of the data were collected in SO analyser software after three good hammer hits and from these, amplitude and peak frequency data were obtained. Peak frequency results are specified in Figure 23.

3.2.4 Data analysis and modal information extraction

The National instrument data analyser software 'SO analyzer' was used to synchronize modal information and to get frequency response function of the structure. At acquisition stage, measurement was taken at 10 different node points so in total 10 FRFs were generated. Advanced MDOF (multi degree of freedom) wizard was used for synchronization and to extract the modal information. It can be seen from the graph (figure 23) that there are several peaks appear because all FRF data were overlapped on each other. All peaks in the graph represent the natural frequencies of the rig. At each frequency the shape of the structure should change. These are the mode shape of the structure. From this graph, first two peak amplitudes from the overlapping graph were picked and frequency and damping values were saved. It should be noted that, if difference between the nearest two damping values are high then it must be error in the curve fitting.

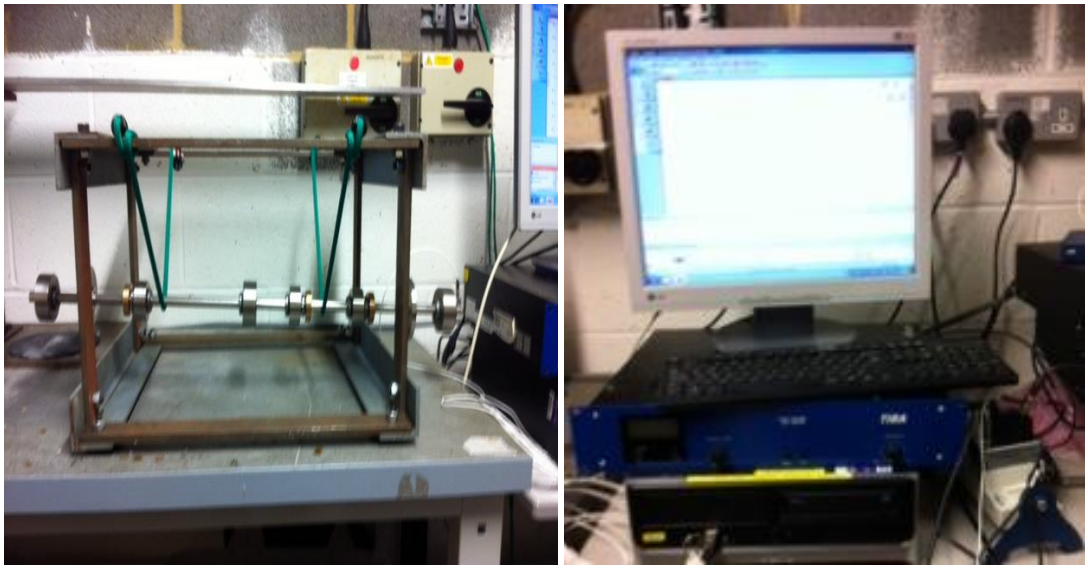

Figure: 20 Experimental impact test set up

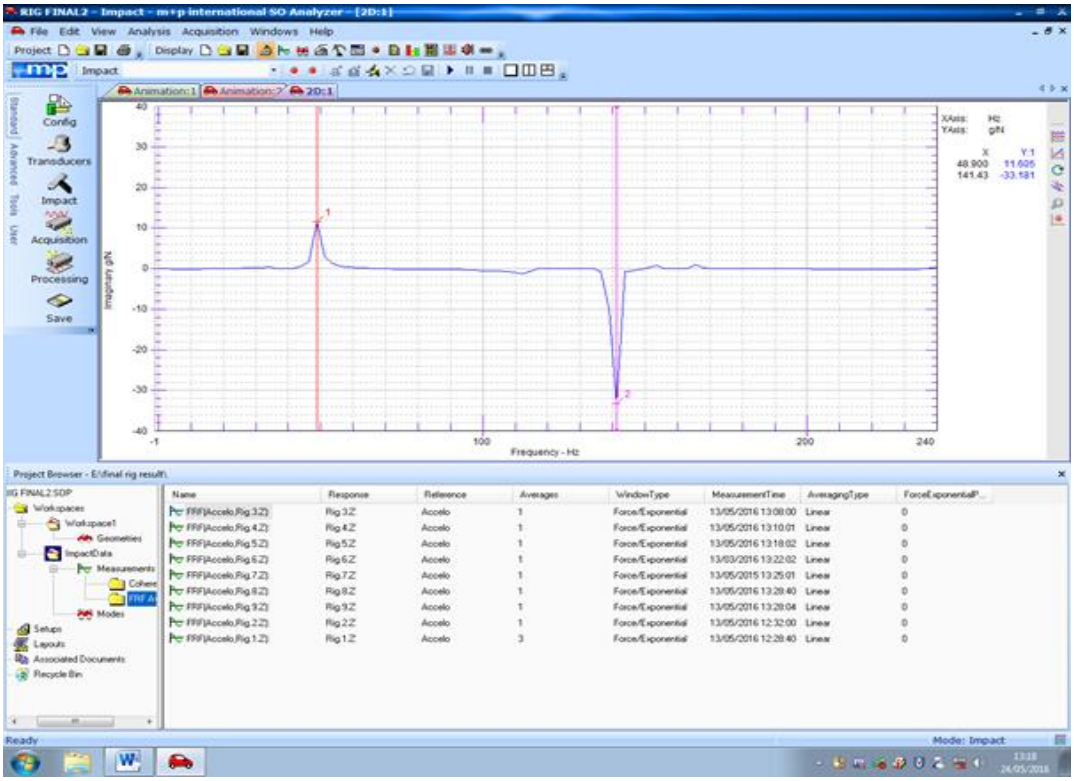

Figure: 21 FRF function of point 3

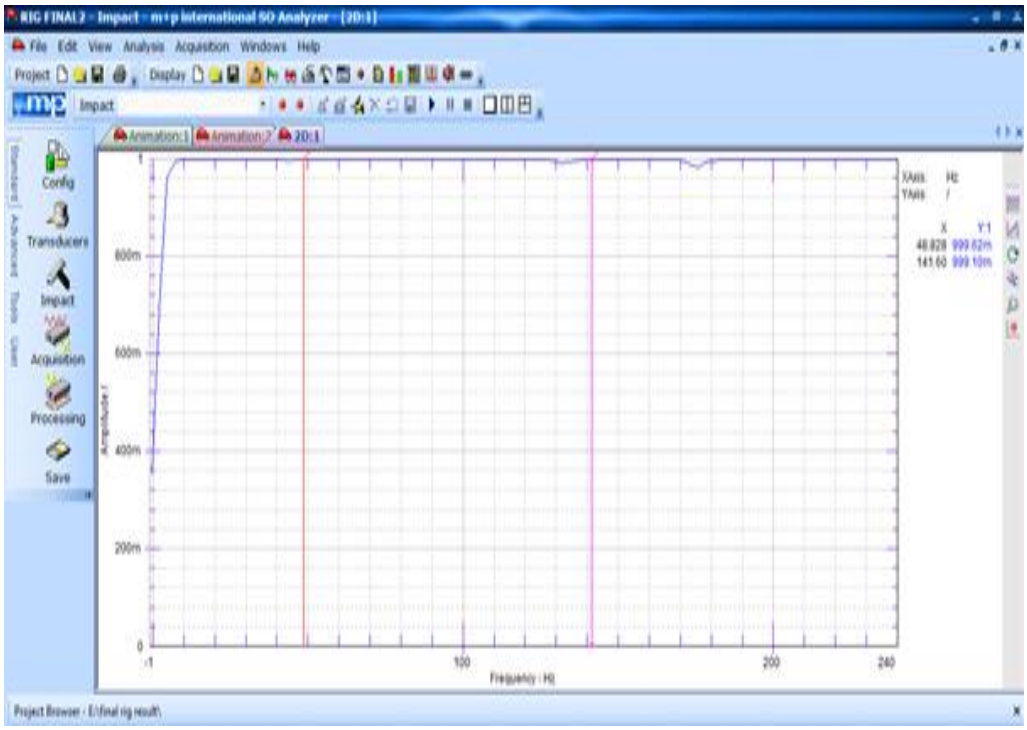

Figure 22 Coherence function of point 3

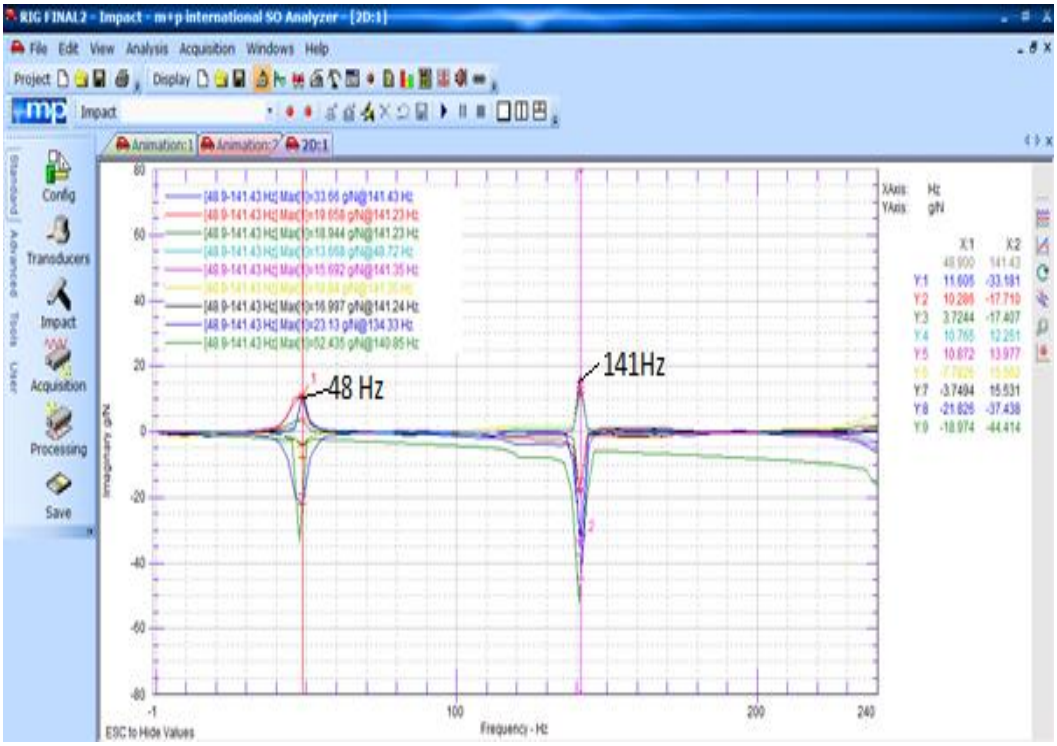

Figure 23: Overlapped FRF's

3.3 Comparison of experimental modal analysis results and FEM model

FEM technique is a powerful technique to identify vibration behaviour of the structure. However, FEM process is based on assumptions; if the physical condition is based on approximation or simplification it might induce errors. Although, simulation results of the new rig are closely matched with MATALAB results, further experimental results helps to verify simulation results. Since the whole rig design is based on the first two mode frequency range, only two mode results are obtained for comparison. Figures: 24-28 show a comparison of first two modes of FEM results, MATALAB results and experimental modal analysis results. From the Table 3.2 and 3.3 it can be stated that both the frequency range differentiate by 5% AND 0.23% due to unnecessary noise in the data, experimental data mode shape curves is smooth enough to predict the behaviour of the rotor.

As evident, finite element flexible rotor model can be considered as an accurate model. In future, further design experiments can be carried out using this model.

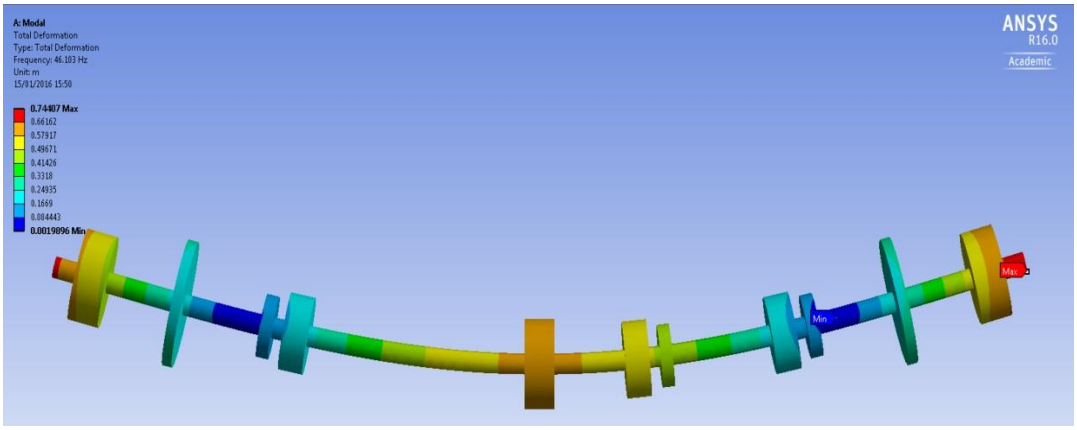

Figure 24: First mode natural frequency Response using FEA at $f_n = 46.2H_Z$

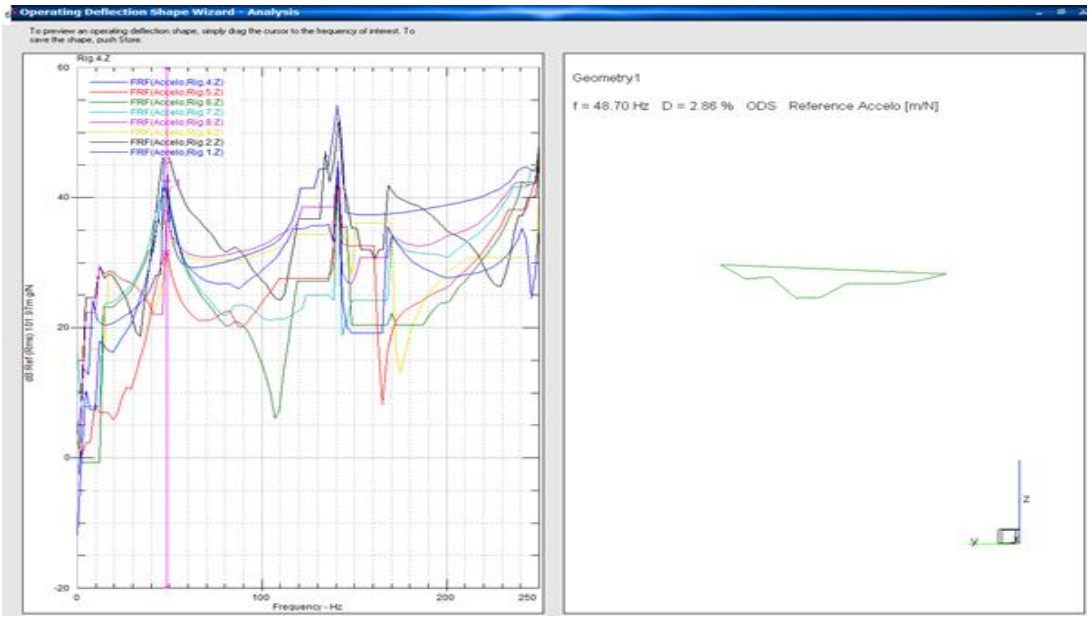

Figure 25: First mode natural frequency response using impact test at $f_n = 48.7H_Z$

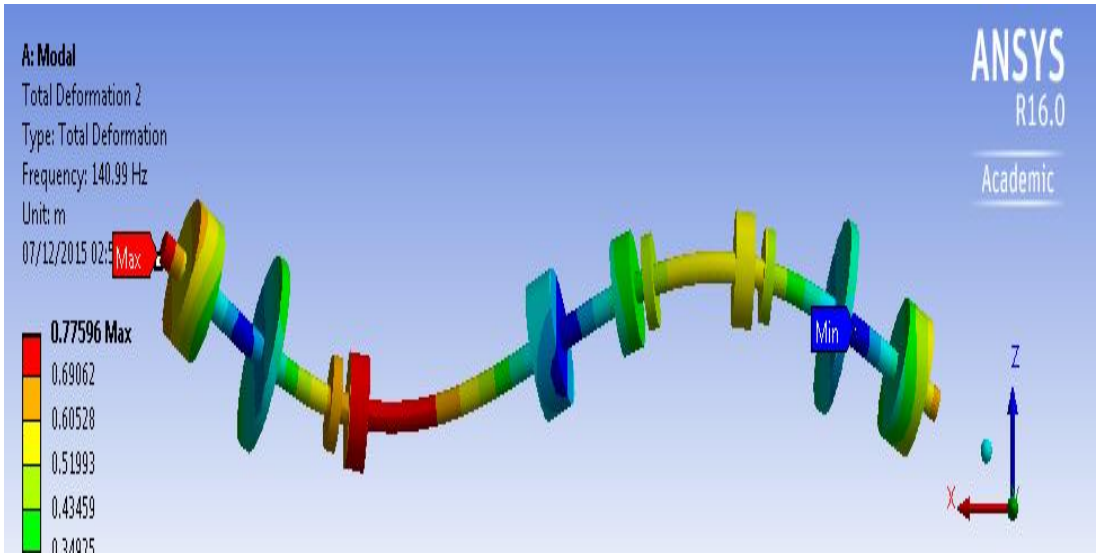

Figure: 26 Second mode natural frequency response using FEA at $f_n = 140.9H_Z$

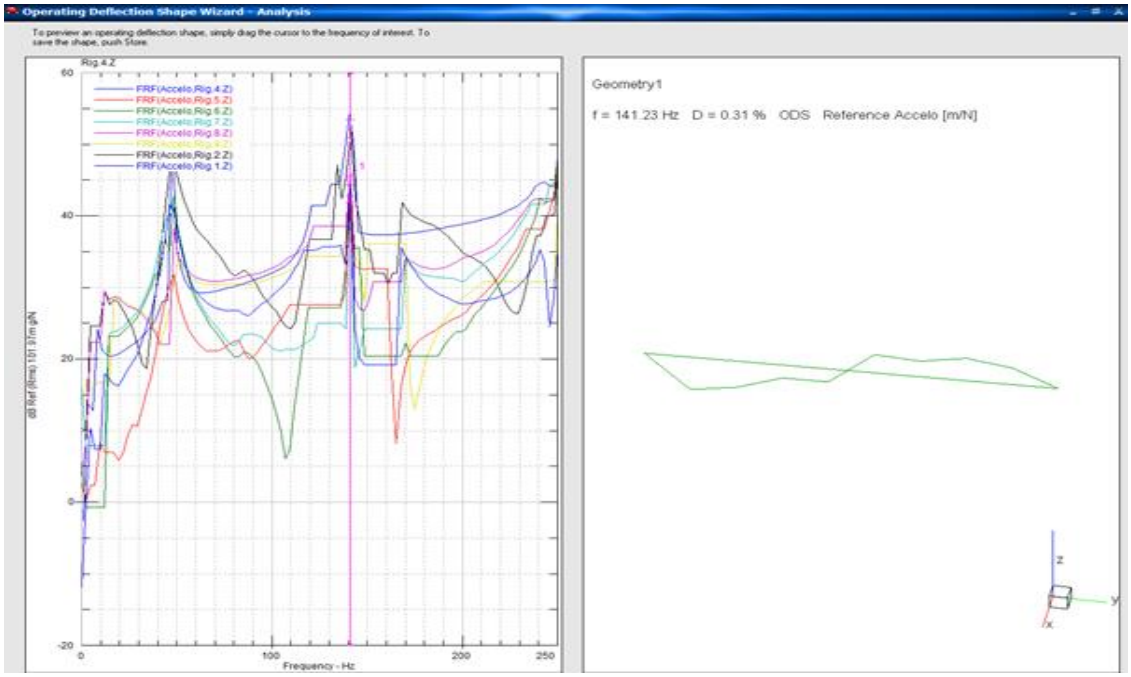

Figure 27: Second mode natural frequency response using impact test at $f_n = 141.23H_Z$

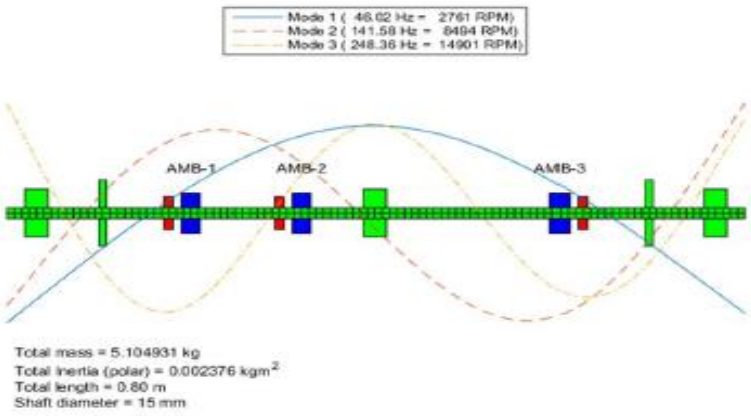

Figure 28: First and Second mode natural frequency response in MATALAB software [77]

Table: 3.2 Comparison between FEA and experimental impact test

Mode	FEA Ansys (Hz)	Experimental Modal test (Hz)	Deviation from test (%)
1	46.2	48.7	5
2	140.9	141.23	0.23

Table: 3.3 Comparison between MATALAB results and experimental impact test

Mode	MATALAB modal analysis	Experimental Modal test (Hz)	Deviation from test (%)
1	46.02	48.7	5
2	141.58	141.23	0.24

3.4 Summary

The aim of the experimental modal analysis was to study the vibration behaviour of the proposed rig model and to prove model accuracy by comparing frequency response results from FEA software with experimental impact test results. Both experimental impact test and simulation results were carried out and results were carefully compared with each other.

The comparison result shows reasonable agreement with the measured frequencies of the bending modes. Slight increase in the bending mode frequencies was expected due to the axial stress caused by accelerometer mounting adhesive. However, this can be improved using other mounting arrangements for accelerometer.

The shape of the magnitude curve from FEA model and experimental test results shows good agreement. However, there is some difference in the shape of the curve. This is due to non-symmetry. The rig model has been built assuming that it is a symmetric structure however the real rig model may have number of asymmetry such as locations of the discs, bearing, and mechanical structure of the rig model. Non-symmetrical reading for the shaft and discs can be seen in figure 25. Further, in FEA geometry is divided in 383 numbers of elements while doing experiment only 10 points are taken. Although, these readings provide enough information to predict the stability and the dynamic behaviour of the rotor from experimental studies, it can be concluded that proposed new rig model is reasonably accurate. Ansys numerical method provides good results for structural modal parameters. In future, this model could be helpful for those who want to do new design experiments. Further test, similar to experimental and simulation tests, can also be performed considering structure's rotational speed and gyroscopic effect.

CHAPTER 4

4.1. Conclusion

In this work computationally efficient design, modelling and simulation of flexible rotor/magnetic bearing system rig has been developed. The new rig has been designed to provide a platform for new research studies to investigate rotor-touchdown contact problems occurring due to large sudden loading in turbo machinery. In addition, design of the test rig was aimed to bring new facility in our university.

As recent industries demands are towards safer, reliable and higher operating speed, it is necessary to obtain dynamic behaviour of the flexible rotor model and it is bending natural frequencies well in advanced. Usually, to predict dynamic behaviour of flexible rotor system model using numeric method is a very complex process therefore in this thesis, finite element optimisation method are used to obtain rotor model configurations and to investigate free-free vibration analysis of the flexible shaft model. The Campbell diagram has been plotted where frequencies were represented as a function of rotational speed. Diagram shows change in the natural frequency over rotational speed and structure shows stable behaviour for the design rotational speed interval.

At the second stage of the project the design of stator, AMB and control parts requirements were carried out. Necessary drawings for all the manufacturing parts were created in Unigraphics. Later, required purchase parts list was made in Excel. Idea was to get rough estimation of the project cost. At later stage, inquiry was sent to three different suppliers and quotations were obtained.

The experimental modal analysis tests undertaken using rotor bearing system model, which provides verification of the simulation technique. Hammer known as force transducer was used in test as excitation of the system and accelerometer used to measure response of the system. First and second mode frequency response values and mode shapes were obtained using impact/hammer test.

Both FEA frequency values were compared and showed good agreement with the simulation results, except small difference in the first mode natural frequency. From both experimental and FEA results it is possible to predict the behaviour of the rotor model and the accuracy of the model has been verified.

4.2 Future work

This thesis work can be further improved in following areas:

The major improvement in this work is the development of the new control method with constrained active magnetic actuator. Going to this aim the dynamic behaviour of the rotor model is proposed and verified. Necessary control parameters are also calculated which will help for the design of controller.

Using MATALAB software, the framework to assemble all system components into analytical model could be obtained for novel control design. Further, rig could be connected with all electrical parts and experiments can be taken to validate control parameters. The quotations obtained in this work could be used to finalize purchase of the electrical system parts.

Magnetic field parameters effect the controller stability therefore early analysis of magnetic field parameters using FEA could be obtained to get the imagination of the effect of magnetic force distribution. AMB drawings and model could be used to do further AMB analysis.

APPENDIX A

Design calculations of radial bearing:

Design Calulation

Mass (Kg)	g		Fmax (N)	Fmax (KN)		u0 (H/m)	Cos22.5		Bmax (T)	Aa m2	Aa Cm2
5.1	9.8		108	0.108		1.256E-06	0.923		1.3	8.68056E-05	0.868056344

$$F_{max} = 6.1 \times \frac{m \times g \times 1.414}{2}$$

$$A_p = \frac{F_{max}}{B_{max}^2} \times \frac{\mu_0}{cos\alpha}$$

$$c = \frac{\pi \times D_i \times 1000}{16}$$

$$F_{ni,max} = \frac{B_{max} \times B_{max}}{\mu_0} \times C_g$$

PI	Di (mm)		C mm	C(m)	b mm	Cg (m)	N	Fni, max	Imax (A)	Max Speed	L (H)	mH	Vmax	P(W)
3.14	56		11	1.10E-02	7.89E+00	0.0005	259	1035	4	10000	0.007313699	7.313699005	15	58.400

Cos22.5	Km (N/M^2/A^2)	g	Fs (N)	Ib (A)	Kx (N/m)	Kc (N/A)	Kbmax (KN/m)
0.923	1.7E-06	9.8	17.51	1.998131	221301.8092	53.9538858	172.62
					221.3018092		

$$b = \frac{a}{c}$$

$$L = \frac{N \times N \times A_a}{2s}$$

$$P = V_{max} \times I_{max}$$

$$V_{max} = L \times \frac{I_{max} \times Max\ Speed}{2}$$

MINIMUM WIRE DIA Calculation:

	Density (A/mm2)	Imax	Wire Dia (mm)	Area Aw (mm2)		Min Wire Dia Choosen mm	Area Choosen mm2	N Turns	Bulk factor	Required Slot Area mm2	Area (An) Cm2	h	C	Available Slot Area
	6	4	0.9	0.7		1	1	259	0.7	370	3.7000000000	35	11	h*c
														385

$$d = \sqrt{I_{max} \times \left(\frac{4}{\rho \times \pi}\right)}$$

$$A_w = \pi \times \frac{d^2}{4}$$

$$A_n = \frac{A_w \times N}{0.7}$$

385>259

APPENDIX B

Design calculations of axial bearing:

Mass (Kg)	Weight (Kg	Fmax	Fmax (KN)	u0	Cg	Bmax	Ap(m^2)	Ap mm2	Fnimax (A-T)	N	Imax (A)	NI (AmpTurn)
5.1	9.8	108	0.108	1.256E-06	0.00075	0.8	0.000212	2.12E+02	1.51E-09	159	4	636

$$F_{max} = 6.1 \times \frac{m \times g \times 1.414}{2} \qquad A_p = \frac{F_{max}}{B_{max}^2} \times \frac{\mu_0}{\cos\alpha} \qquad F_{NI} = 2 \times \mu_0 \times C_g \times B_{max}$$

d1 mm	d mm	c1mm	da mm	d2 mm	c2 mm	c3 mm	bd mm	N	An mm2	c4 mm	c5 mm
47.90	45	1.45	90	88.49	0.75	1.41	11.5	159	227.14	20.29	11.19

$$c_1 = \frac{d_1 - d_2}{2} \qquad c_2 = \frac{d_a - d_2}{2} \qquad c_4 = \frac{d_2 - d_1}{2}$$

APPENDIX C

Design drawings of active magnetic bearing assembly components:

Rotor Shaft Drawing

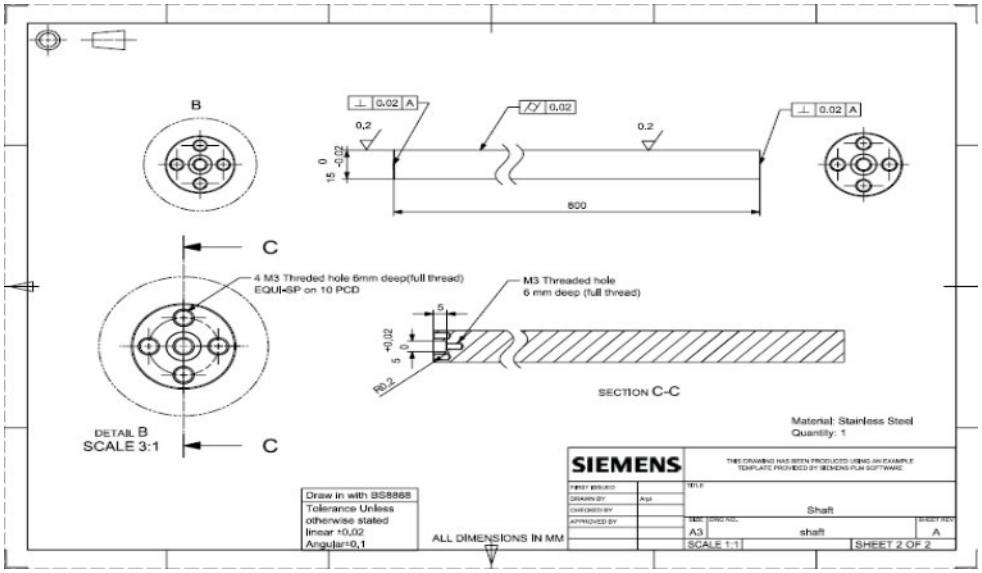

Rotor Laminations sheet drawing

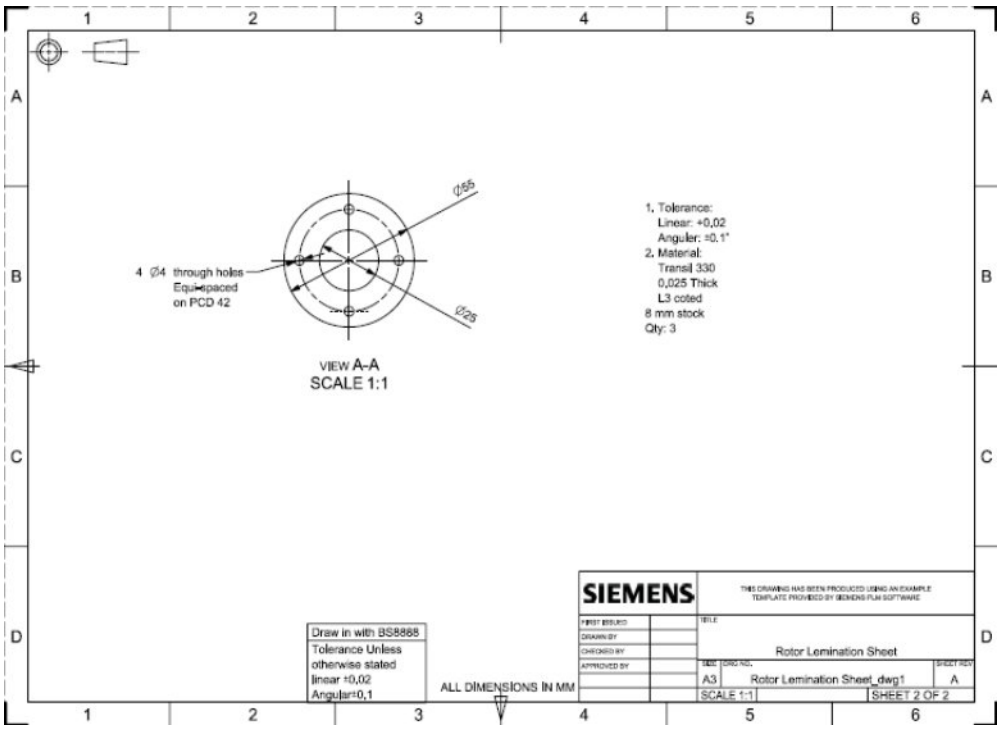

Stator lamination coil drawing

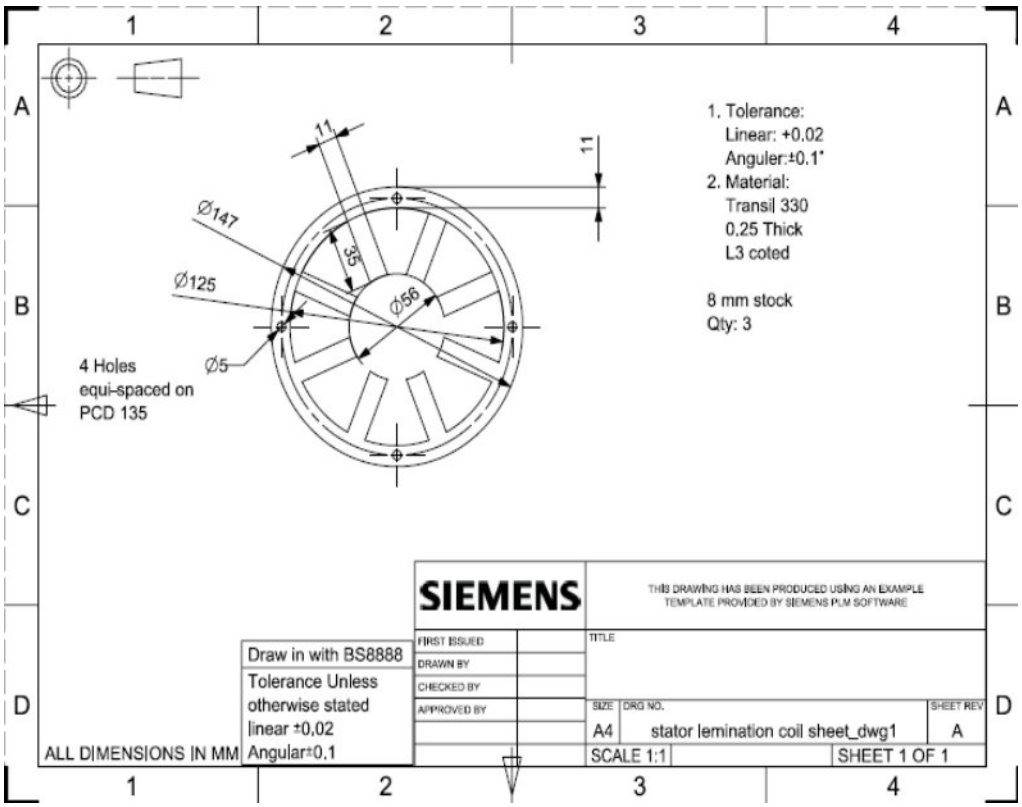

Touchdown bearing disc

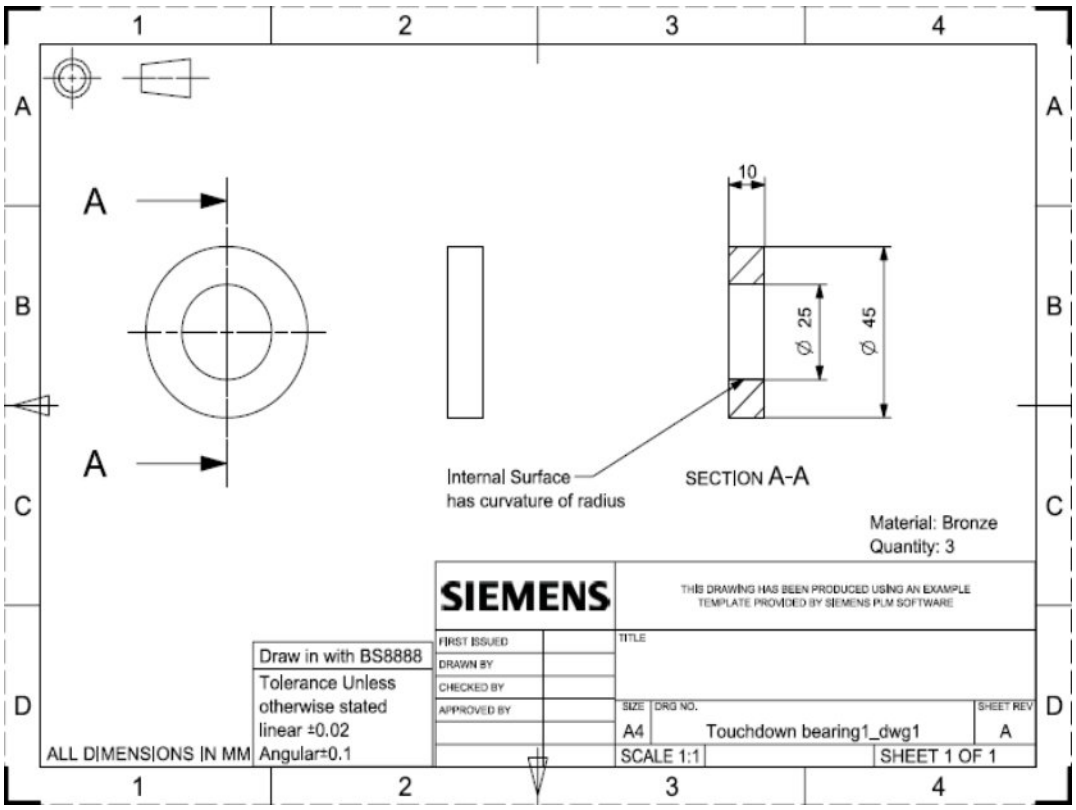

Middle Disc

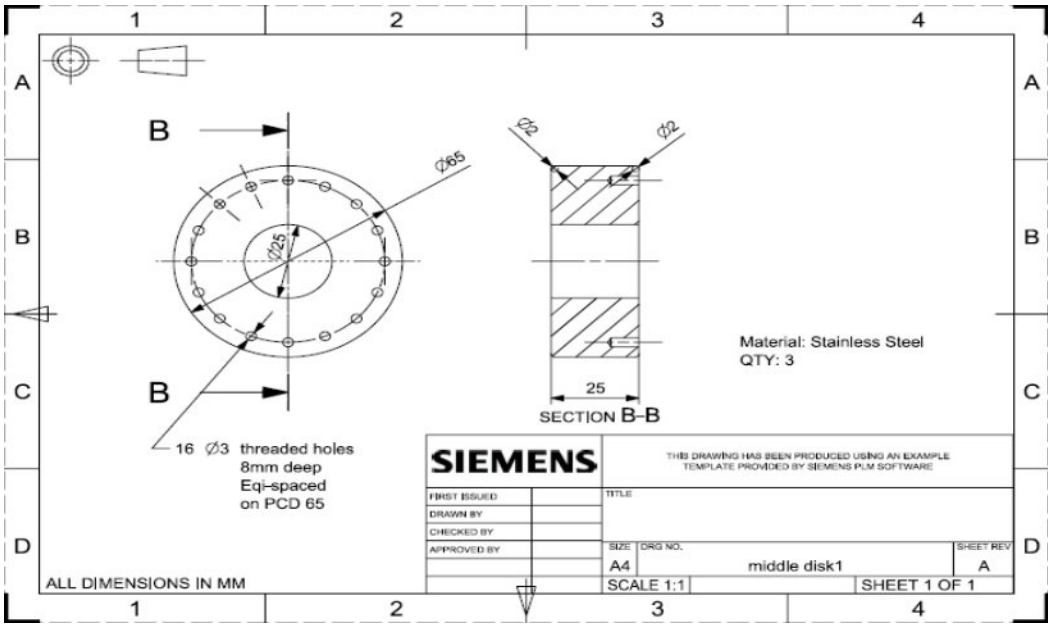

References

1. S. Earnshaw (1842) "On the nature of the molecular forces which regulate the constitution of the luminiferous ether," *Trans. Camb. Phil. Soc*, vol. 7, pp. 97- 112

2. W. Brown Beck (1939) "Levitating body in electric and magnetic field," *Z. Phys* 112, 753

3. Schwitzer, G. & Maslen, E. H (2009) "*Magnetic Bearings Theory, Design, and Application to rotating machinery Handbook*," e-ISBN 978-3-642-00496-4, Springer, p. 535, London

4. Schweitzer, G (2002) "Active magnetic bearings – Chances and Limits," *Proceeding of the 6th Internat. IFToMM Conf. on Rotor Dynamics*, Sydney.

5. J.C Ji, Colin H. Hansen, Anthony C. Zander (2008) "Nonlinear Dynamics of Magnetic Bearing Systems" *Journal of Intelligent Material Systems and Structures*, 19(12), pp.1471-1491

6. Swanson, E. and Hawkins, L (2014) "New Active Magnetic bearing Requirement for compressor in API 617 eight edition". *In the Proceedings of the 43rd Turbomachinery Symposium*, 22-25, Sep. Houston, Texas

7. Alves, P (1998) "Magnetic Bearing- A Primer". *In Proceeding of the 27th turbo-machinery Synonymous*. pp. 1-5, Calgary, Canada.

8. Swanson, E. E. & Maslen, E. H. & Li, G. & Cloud C. H (2008) "Rotordynamic design audits of AMB supported machinery" *Proceedings of the Thirty-seventh Turbomachinery Symposium*" September. Virginia

9. ISO standard (2002) ISO 14839-1: "Mechanical vibration – Vibration of rotating machinery equipped with active magnetic bearings – Part 1:" *1st edition. Genève: International Organization for Standardization"*, p. 30.(Accessed : 09 may 2015)

10. M. N. Sahinkaya, A. G. Abulrub, and P. S. Keogh (2004) "On the modeling of flexible rotor/magnetic bearing systems when in contact with retainer bearings," *presented at the 9th Int. Symp. Magn. Bearings (ISMB9)*, Lexington, KY.

11. Lantto E (1999) “Robust control of magnetic bearing in subcritical machines”, *Acta Polytechnica Scandinavica*, *Electrical Engineering Series No. 94*, pp 143

12. Kim, H. and Lee, C (2006) “Design and control of an active magnetic bearing system with Lorentz force-type axial actuator”. *Mechatronics*, 16(1), pp.13-20.

13. Yoo, S., Lee, W., Bae, Y. and Noh, M (2010) “Design of magnetically levitated rotors in a large flywheel energy storage system from a stability standpoint”. *Journal of Mechanical Science and Technology*, 24(1), pp.231-235.

14. Calnetix (2016) *Advantages of Magnetic Bearings*. 2015-2016 [online]. Available at: http://www.calnetix.com/resource/magnetic-bearings/advantages-magnetic-bearings. [Accessed 16 Apr. 2016].

15. Abulrub, A. H. G., Sahinkaya, M. N., Burrows, C. R., and Keogh, P. S.(2009) “Performance Assessment of a Multi-Frequency Controller Applied to a Flexible Rotor Magnetic Bearing System—Contact Dynamics,” *Motion and Vibration Control*, H. Ulbrich and L. Ginzinger, eds., Springer, Dordrecht, the Netherlands, pp. 11–20.

16. L. Burdet (2006) “Active Magnetic Bearing Design and Characterization for High Temperature Applications”, Thèse N°3616, EPFL, Lausanne.

17. Kasarda, M (2000) “An Overview of Active Magnetic Bearing Technology and Applications”. *The Shock and Vibration Digest*, 32(2), pp.91-99

18. Clark DJ, Jansen MJ and Montague GT (2004) “An overview of magnetic bearing technology for gas turbine engines”. *NASA report /TM-2004-213177*, Available at ntrs.nasa.gov/archive/nasa/casi.ntrs.nasa.gov/20040110826.pdf (Accessed : 09 may 2015)

19. Zmood R, Pang D., Anand D., Kirk J (1990) “Robust Magnetic Bearings for Flywheel Energy Storage Systems”, pp. 123-129, Tokyo, Japan.

20. Ji, J., Hansen, C. and Zander, A (2008) “Nonlinear Dynamics of Magnetic Bearing Systems”. *Journal of Intelligent Material Systems and Structures*, 19(12), pp.1471-1491.

21. Keogh, P.S., Cole, M.O.T., and Burrows, C.R (2002) “ Multi-state transient rotor vibration control using sampled harmonics”, *Transactions of the ASME Journal of Vibration and Acoustics*, vol.124, pp.186-197

22. M. Montiel, G. Montiel, A. García (2014) “Active Vibration Control in a Rotor System by an Active Suspension with Linear Actuators”. *Journal of Applied Research and Technology* 12, pp 898–907

23. Yun, S., Lin, Z. and Allaire, P (2013) “Control of surge in centrifugal compressors by active magnetic bearings”, Springer, London

24. Mohammad Hadi Jalali, Behrooz Shahriari, Mostafa Ghayour, Saeed Ziaei-Rad, Shahram Yousefi (2014) “ Evaluation of Dynamic Behavior of a Rotor-Bearing System in Operating Conditions”, Vol:8 No:10 pp-1599-1600

25. Elhiber, S. (2009) “Dynamic analysis of a rotor bearing system”. Bachelor of Science thesis. Cleveland State University. Available at https://etd.ohiolink.edu/rws_etd/document/get/csu1245868731/inline.pdf. (Accessed : 09 may 2015)

26. R. Gasch (1976) “Vibration of large turbo rotors in fluid-film Bearing on an elastic foundation”, *Journal of Sound and Vibration*, Vol. 47, pp.53-73.

27. J.M. Vance, B.T. Murphy and H.A. Tripp (1987) “Critical speeds of turbomachinery: computer predictions vs. experimental measurements – Part II: effect of tilt-pad Bearing and foundation dynamics”, *ASME Journal of Vibration Acoustics, Stress, Reliability in Design*, Vol. 109, pp.8-14.

28. R.G. Kirk and E.J. Gunter (1972) “The effect of support flexibility and damping on the synchronous response of a single-mass flexible Rotor”, *ASME Journal of Engineering for Industries*, Vol. 94, pp.221-232.

29. Miranda, W. and Faria, M (2014) “Finite Element Method Applied to the Eigenvalue Analysis of Flexible Rotors Supported by Journal Bearings”. *Engineering*, 06(03), pp.127-137

30. Lee et al, F.-Z. Hsiao, D. Ko (1994) “Analysis and testing of magnetic bearing with permanent magnets for bias”, *ISME International Journal, Series C*, vol. 37, No. 4, pp. 774-782.

31. Habermann and Brunet (1984) “The active magnetic bearing enables optimum damping of exible rotor”, *ASME Paper No. 84-GT-114*.

.

32. Han W. S., Lee C. W, and Okada Y (2002) “Design and control of a disk-type integrated motor-bearing system”, *IEEE/ ASME Trans. on Mechatronics*, 7(1):15-22, Mar.

33. Okada Y., Konishi H., Kanebako H.,and Lee C. W (2000) “Lorentz force type self-bearing motor”, *Proc. 7th Int. Symp. Magnetic Bearings*, pp.353-358, Aug. ETH, Zurich.

34. Wei Kang, Borges, C. and Mingqing Xiao (2003) “Symposium on new trends in nonlinear dynamics and control and their applications”, *IEEE Control Systems*, 23(3), pp.99-100.

35. M. MacCamhaoil (No date) Static and Dynamic Balancing of Rigid Rotors. Bruel & Kjaer application notes. BO 0276-12 Available at: http://www.bksv. com/doc/BO0276.pdf. (Accessed : 09 may 2015)

36. M Waseem (2015) “Diagnosis of active magnetic bearing system faults using principal component analysis”, *International Journal of Advances in Engineering & Scientific Research*, Volume 2, Issue 1, pp 36-42

37. Li, P. 2015 “Active touchdown bearing control in magnetic bearing system”. PhD. Thesis, University of Bath. Available at opus.bath.ac.uk/45120/1/thesis_final.pdf. (Accessed : 09 may 2015)

38. S. Başaran1 , S. Sivrioğlu1 , B. Okur1,2 and E. Zergeroğlu (2011) “Robust H Control of Flexible Rotor Active Magnetic Bearing System”, *on the proceeding of 6th International Advanced Technologies Symposium (IATS’11)*, pp 16-18, Elazığ, Turkey.

39. Kärkkäinen, A., Sopanen, J. and Mikkola, A (2006) “*Simulation of AMB supported rotor during drop on retainer bearing*”. *ISBN 952-214-201-8*. Lappeenranta University of Technology. Finland

40. Ishii, T., and Kirk, R. G (1996) “Transient Response Technique Applied to Active Magnetic Bearing Machinery during Rotor Drop,” *ASME Journal of Vibration and Acoustics*, 118, pp. 154-163

41. Xie, H., Flowers, G.T., Feng, L., and Lawrence, C (1999) “Steady-state dynamic behaviour of a flexible rotor with auxiliary support from a clearance bearing”, *Transactions of the ASME Journal of Vibration and Acoustics*, vol.121 (1), pp.78-83.

42. Cole, M.O.T., Keogh, P.S., and Burrows, C.R (1998) "Vibration control of a flexible/magnetic bearing system subject to direct forcing and base motion disturbances", *Proceedings of the Institution of Mechanical Engineers Part C-Journal of Mechanical Engineering Science*, vol.212(7), pp.535-546

43. Cole, M.O.T., and Keogh, P.S (2003) "Rotor vibration with auxiliary bearing contact in magnetic bearing systems, Part 2: robust synchronous control for rotor position recovery", *Proceedings of the Institution of Mechanical Engineers Part C-Journal of Mechanical Engineering Science*, vol.217, pp.393-409

44. Raju, K. V. S., Ramesh, K., Swanson, E. E., and Kirk, R. G (1995) "Simulation of AMB Turbomachinery for Transient Loading Conditions," *Proceedings of MAG'95*, *Alexandria*, *USA*, *August*, *Technomics Publishers Co.*, pp. 227-235,

45. Fawaz Y. Saket, M. Necip Sahinkaya and Patrick S. Keogh (2015) "Experimental Assessment of Touchdown Bearing Contact Forces in Magnetic Bearing Systems", *Proceedings of the 9th IFToMM International Conference on Rotor Dynamics*, *Mechanisms and Machine Science 21*, DOI 10.1007/978-3-319-06590-8_123

46. Palazzolo, A. B., Lin, R. R., Alexander, R. M., Kascak, A. F., and Montague, J (1991) "Test and theory for piezoelectric actuator-active vibration control of rotating machinery" *Trans. ASME J. Vibr. Acous*, 113(2), pp 167–175

47. Li, G., Lin, Z., Allaire, P. E., Huang, B., Jiang, W., Zorzi, S. E. and Bartlett,R. O (2001) "Stabilization of a High Speed Rotor With Active Magnetic Bearings by a Piecewise-Synthesis Controller, *"Proc. of the 6th Int. Symp. On Magnetic Suspension Technology*, Turin, Italy,

48. L. Zhu, C. Knospe, and E. Maslen (2004) "Frequency domain modeling of nonlaminated C-shaped magnetic actuators," *in Proc. 9th Int. Symp. Magn. Bearings*, pp. 1–6, Lexington, KY

49. li, P., Sahinkayaa, N. and Keogha, P (2014) " Active Touchdown Bearing Control for Recovery of Contact-Free Rotor Levitation in AMB Systems". *In: ISMB14*, *14th International Symposium on Magnetic Bearings*, pp.11-14, Linz, Austria

50. Welse,D. A and Pinckney.F,D (2014) "An introduction and case history review of active magnetic bearing", *Proceedings of the eighteenth turbomachinery symposium*, The Turbomachinery Laboratory, The Texas A&M University System, 1989. Texas

51. Barbaraci, G (No date)“ Axial active magnetic bearing design”, Journal of Vibration and Control, 22(5), pp.1190-1197

52. Biswas, P.K., Banerjee, S (2013) “ANSYS based fem analysis for three and four coil active magnetic bearing-a comparative study”, *International Journal of Applied Science and Engineering* 11(3): 277-292

53. Al-Khazali, H. and Askari, M. (2012). ‘’The Experimental Analysis of Vibration Monitoring in System Rotor Dynamic with Validate Results Using Simulation Data’’, *ISRN Mechanical Engineering*, pp.1-17.

54. He, J. and Fu, Z. (2001). *Modal analysis*. Oxford: Butterworth-Heinemann.

55. Mpihome.com (2016). *Noise & Vibration Testing – m+p international - m+p international - English*. [online] Available at: https://www.mpihome.com/ [Accessed 18 May 2016].

56. De Silva, C. (2005). *Vibration and shock handbook*. Boca Raton: Taylor & Francis.

57. Wang, Y. (2015). *Vibrational measurement techniques applied on FE-model updating*. MSc thesis. Linnaeus University, Faculty of Technology.

58. Modalshop.com. (2016*). The Fundamental of the modal testing*. [online] Available at: http://www.modalshop.com/ [Accessed 9 May 2016].

59. Endevco.com. (2016). *Steps to selecting the right accelerometer*. [online] Available at: https://www.endevco.com [Accessed 18 May 2016].

60. Lds-group.com. (2003). *Basics of Structural Vibration Testing and Analysis*. [online] Available at: http://www.lds-group.com/ [Accessed 19 May 2016].

61. Lu, Y. (2013). *Comparison of Finite Element Method and Modal Analysis of Violin Top Plate*. Master of Arts in Music Technology. McGill University.

62. Childs, D (1993) *Turbomachinery Rototordynamics*, John Wiles & Sons, Inc; New York

63. Kramer, E. (1993) *Dynamics of Rotor and Foundations*, Springer-Verlag, New York

64. Genta, G (2005) *Dynamics of Rotor system*, Springer.

65. Mohiuddin, M.A., Bettayeb, M., Khulief, Y.A. (1998), “Dynamic analysis and reduced order modeling of flexible rotor-bearing systems”. *Computers and Structures*, Vol.69, pp349-359.

66. R.W. Stephenson and K.E. Rouch (1992). ‘’Generating matrices of the foundation structure of a Rotor system from test data’’. *Journal of Sound and Vibration*, Vol. 154, pp.467-484.

67. Seok-Myeong Jang, Un-Ho Lee, Jang-Young Choi, and Jung-Pyo Hong (2008), “Design and analysis of thrust active magnetic bearing”. *Journal of Applied Physics*, Vol. 103, pp. 07F122 - 07F122-3, April

68. Horikawa, O., and I. da Silva (2002). "Single axis controlled attraction type magnetic bearing". *Journal of the Brazilian Society of Mechanical Sciences*, 24.4: 324-329.

69. Zeng, S. (2002), “Motion of AMB Rotor in Backup Bearings”. *ASME Journal of Vibration and Acoustics*, 124, pp. 460-464.

70. Ecker, H. (1998),”Nonlinear Stability Analysis of a Single Mass Rotor Contacting a Rigid Backup Bearing”. *Proceedings of the Euromech Colloquium*: 15-18 September, Loughborough, United Kingdom, September, Springer Verlag, pp. 79-89.

71. Swanson, E. E., Kirk, R. G., and Wang, J., (1995) “AMB Rotor Drop Initial Transient on Ball and Solid Bearings”. *Proceedings of MAG'95*, *Alexandria*, USA, August, Technomics Publishers Co., pp. 207-216.

72. Wang, X., and Noah, S., (1998) “Nonlinear Dynamics of a Magnetically Supported Rotor on Safety Auxiliary Bearings”. *ASME Journal of Vibration and Acoustics*, 120, pp. 596-606.

73. Sahinkaya, M. N., Cole, M. O. T., and Burrows C. R (2001). ‘’Fault detection and tolerance in synchronous vibration control of rotor-magnetic bearing systems’’. *Proc. IMechE*, *Part C: J. Mechanical Engineering Science*, 215(C12), 1401–1416. DOI: 10.1243/0954406011524775.

74. Siegwart R., Larsonneur R., Traxler A. (1990). ‘’Design and Performance of a High Speed Milling Spindle in Digitally Controlled Active Magnetic Bearings’’, *Proceeding of the 2nd International Symposium on Magnetic bearing*, July 12-14, Tokyo, Japan, pp. 197-204.

75. Huang, T., Chen, Z., Zhang, H. and Ding, H. (2015). Active Control of an Active Magnetic Bearings Supported Spindle for Chatter Suppression in Milling Process. *J. Dyn. Sys., Meas., Control*, 137(11), p.111003.

76. Synchrony.com. (2016). *Synchrony AMB from Dresser-Rand How Magnetic Bearings Work.* [online] Available at: http://www.synchrony.com/knowledge/how-magnetic-bearings-work.php [Accessed 8 Jun. 2016].